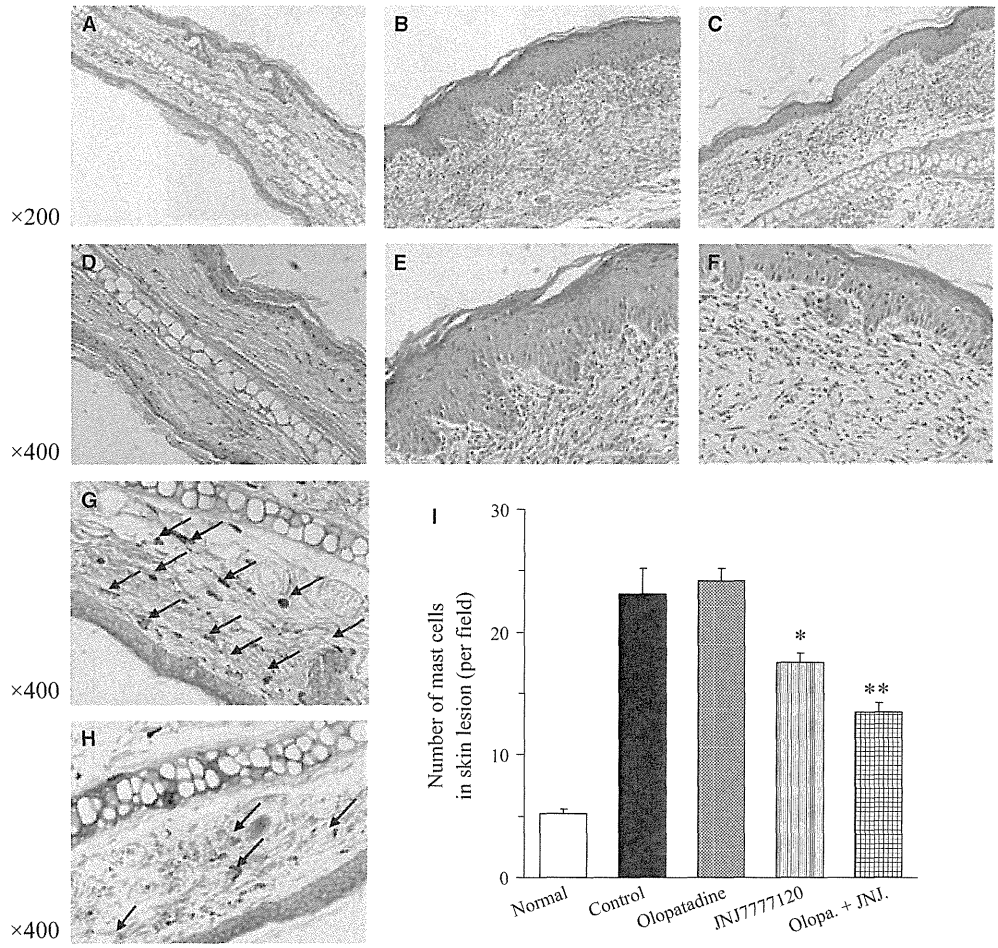

Figure 2 Effects of olopatadine and JNJ7777120 on histological changes in mice treated repeatedly with picryl chloride (PiCl). Ten weeks after the sensitization, skin specimens prepared from intact mice (normal group; A, D), PiCl-treated mice (control group; B, E), and PiCl-treated mice administered olopatadine plus JNJ7777120 (C, F) were stained with hematoxylin and eosin and observed with a light microscope at magnification ×200 (A, B, C) and ×400 (D, E, F). The skin specimens prepared from PiCl-treated mice (G) and PiCl-treated mice administered olopatadine plus JNJ7777120 (H) were stained with toluidine blue, and the numbers of mast cells were counted from four fields with a light microscope ×400 (I). Statistical significance; $*P < 0.05$ and $**P < 0.01$ *vs* control group ($n = 4$–5).

factor of neuronal elongation. The expression of H1R was detected by real-time PCR, but H4R was not detected in unstimulated and histamine-stimulated PAM212 cells (data not shown). The level of mRNA for Sema3A was decreased by histamine at 10 μM (Fig. 5A). The level reached a minimum at 3 h and slowly recovered over the next 9 h (Fig. 5B). The histamine-induced reduction in the level of Sema3A mRNA was antagonized by olopatadine (Fig. 5C) but not by JNJ7777120 at 30 μM (data not shown).

Discussion

In this study, we demonstrated that the H1R antagonist olopatadine and H4R antagonist JNJ7777120 improved scratching behavior and skin inflammation in a model of chronic allergic dermatitis established in NC/Nga mice. The effectiveness of the combined treatment against the dermatitis was almost equal to that of prednisolone.

Skin aberrations such as erythema, lichenification, and erosion accompanied the scratching behavior. The findings that histamine level in plasma and mRNA level for HDC in skin tissue were elevated in mice with chronic inflammation suggested histamine to be involved in the development of chronic allergic dermatitis in this model. As plasma histamine levels were reported to be significantly higher in patients with AD than controls (23, 24), this NC/Nga-based model of chronic dermatitis is an important tool for studying the roles of histamine in AD.

Recently, the anti-allergic effects of H4R antagonists were mainly evaluated in dermatitis model in mice (13, 17–19). Rossbach et al. (17) reported that a combination of H4R and H1R antagonism has prophylactic effects on acute hapten-induced scratching, but not chronic dermatitis. Only the study by Suwa et al. (19) was evaluated therapeutic effects for a H4R antagonist, but is not evaluated about benefits on combined treatment of a H1R and a H4R

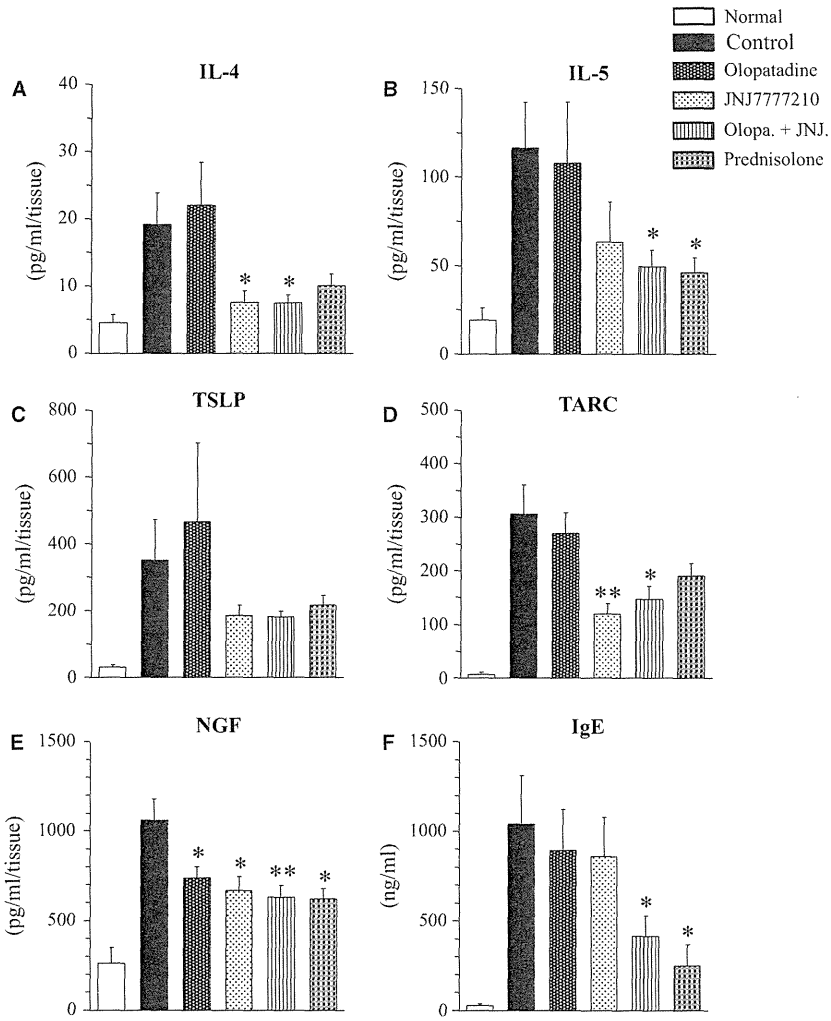

Figure 3 Effects of olopatadine and JNJ7777120 on tissue cytokines and plasma IgE levels in picryl chloride (PiCl)-induced chronic allergic dermatitis. Ten weeks after the sensitization, the levels of cytokines (A–D), nerve growth factor (NGF) (E) in inflamed skin and total IgE in plasma (F) were determined. Statistical significance; $*P < 0.05$ and $**P < 0.01$ *vs* control group ($n = 6$–10).

antagonist. In our study, we first clarified with the therapeutic efficacies in chronic dermatitis, administered both H1R and H4R antagonists. In our model of chronic dermatitis, a H4R antagonist suppressed the PiCl-induced scratching behavior and, combined with a H1R antagonist, had an additive effect as reported in an acute inflammatory model by Rossbach et al. and chemical-induced pruritus model by Dunford et al. (16). As Thurmond et al. (25) suggested that both H1R and H4R are expressed on C-afferent fiber terminals, these drugs might inhibit directly the transmission of itching responses from the peripheral to central nervous system. In addition, we found that both olopatadine and JNJ7777120 reduced the level of NGF in skin lesions. It has been reported that the level of NGF reflected the severity of itching and eruptions in AD (26, 27) and changed the correlation with clinical conditions in olopatadine-treated patients (27). Histamine also induced the production of NGF via H1R in human keratinocytes (28). Our findings suggested that H4R as well as H1R was involved in the production of NGF, resulting in the increase in innervation in the epidermis.

Conversely, Sema3A expression was found to be decreased at the horn layer with immunohistological staining in the skin lesions of patients with AD (29). The decrease in the expression of Sema3A in the inflamed skin was also observed in our model (data not shown). In addition, decrease in Sema3A mRNA in the epidermis from *Dermatophagoides farinae*-induced chronic dermatitis in NC/Nga mice was recovered by olopatadine (30). In this study, we found that histamine decreased the level of Sema3A and olopatadine blocked this reduction in mouse keratinocytes. Because human keratinocytes also express H4R (31), the expression of Sema3A in human keratinocytes might possibly be regulated by H4R as well as H1R. To confirm this possibility, we have now begun studying it using mouse and human primary keratinocytes. These findings indicated that histamine acting via H1R and H4R induces the pruritus in chronic skin inflammation through

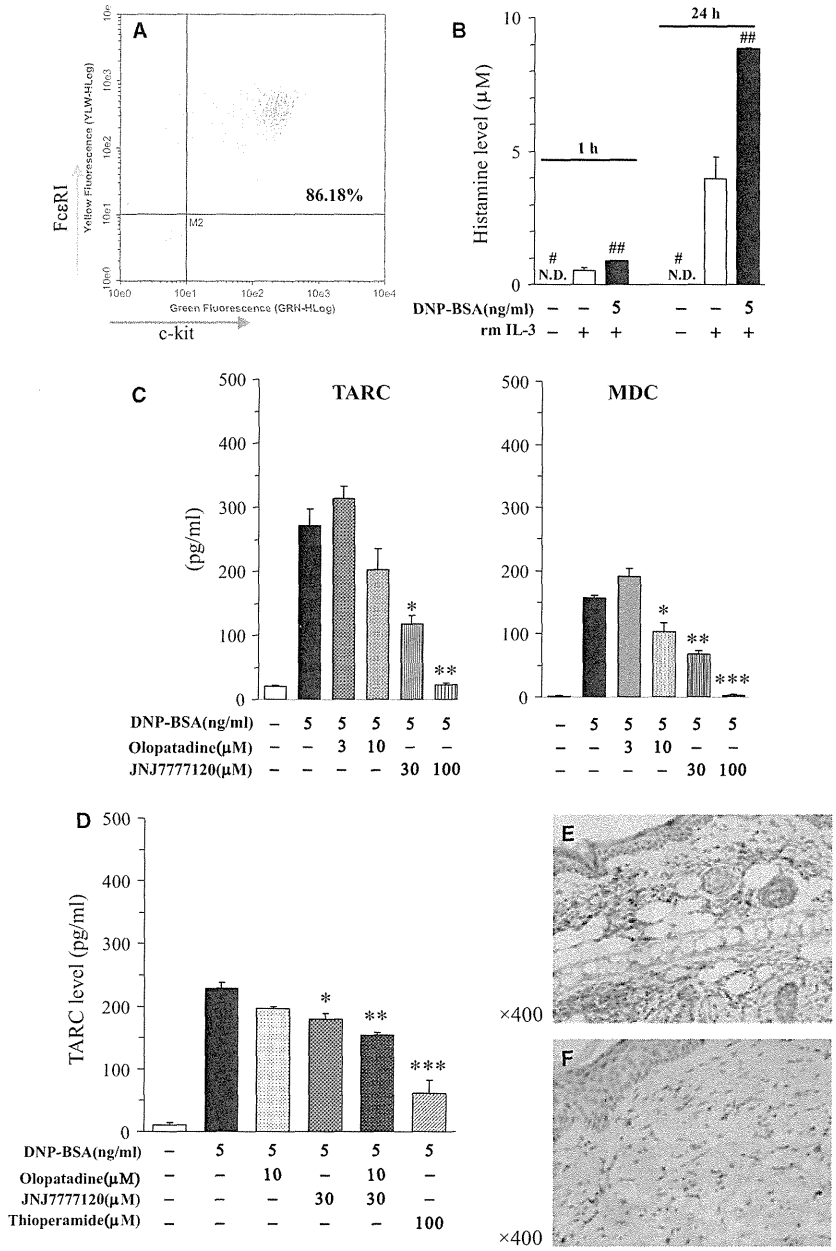

Figure 4 Effects of olopatadine and JNJ7777120 on production of thymus and activation-regulated chemokine (TARC) and macrophage-derived chemokine (MDC) by antigen-stimulated bone marrow-derived mast cells (BMMC) and infiltration of CD4-positive cells in the skin lesions. (A) Bone marrow cells freshly prepared from NC/Nga mice were cultured with IL-3 (300 pg/ml) for 9 days and the expression of FcεRI and c-kit was confirmed by flow cytometry. (B) BMMC were primed overnight with 0.5 μg/ml of DNP IgE and then stimulated with DNP-BSA at the indicated concentrations. The level of histamine (1 and 24 h) in the supernatant was determined. Statistical significance; $^{\#}P < 0.05$ and $^{\#\#}P < 0.01$ *vs* unstimulated. (C, D) The cells were treated with olopatadine, JNJ7777120 and thioperamide for 30 min, and then stimulated with DNP-BSA for 24 h. $^{*}P < 0.05$, $^{**}P < 0.01$ and $^{***}P < 0.001$ *vs* DNP-BSA stimulation. (E, F) Using the tissue specimens in Fig. 2, the CD4-positive T cells that had infiltrated the skin lesions in picryl chloride (PiCl)-treated mice were revealed by immunohistological staining (control group, E; olopatadine and JNJ7777120-administered group, F).

multiple mechanisms and that the combination of H1R and H4R antagonists has additive anti-pruritus effects.

Previously, we reported that the H3R/H4R antagonist thioperamide ameliorated ear swelling in mice with TPA-modified hapten-induced allergic dermatitis, and in combination with the H1R antagonist pyrilamine suppressed the biphasic allergic response: the early phase in which vascular permeability is increased by the degranulation of

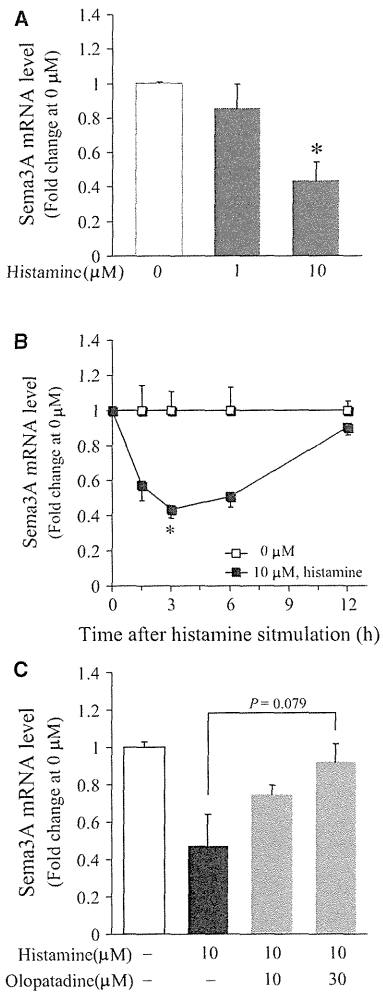

Figure 5 Effects of olopatadine on histamine-induced down-regulation of semaphorin 3A (Sema3A) expression in PAM212 cells. PAM212 cells were cultured with various concentrations of histamine for 3 h, and the level of mRNA for Sema3A was determined by real-time PCR (A). Changes in the level of Sema3A mRNA after the histamine treatment were also measured (B). The cells were cultured for 30 min in medium containing olopatadine and stimulated with histamine at 10 μM for 3 h (C). The level of mRNA is indicated as the fold difference normalized to the unstimulated control. Statistical significance; $*P < 0.05$ *vs* histamine at 0 μM.

mast cells and the late phase which is associated with infiltration by eosinophils and T cells (12). Here, we indicated that chronic allergic dermatitis was also clearly improved by a H1R antagonist plus H4R antagonist (Figs 1 and 2) with almost the same effect as prednisolone (Fig. 1). The effect of the combined treatment on the number of mast cells in skin lesion was also similar to that of prednisolone, which significantly decreased the infiltration of mast cells in skin lesion treated with PiCl repeatedly (32).

JNJ7777120 alone significantly inhibited the production of Th2 cytokines in the skin lesions (Fig. 3). We found that JNJ7777120 markedly inhibited the production of TARC and MDC by antigen-stimulated BMMC. BMMC significantly secreted histamine on stimulation with IgE and then produced TARC and MDC, which are chemokines acting through the CCR4 mainly expressed by Th2 cells. JNJ7777120 inhibited the production of TARC and MDC without inhibiting histamine release. Because BMMC have H4R but not H3R (8), the inhibitory actions of thioperamide could be attributed to H4R antagonism. The inhibition of TARC and MDC production by olopatadine, at least a part, is assumed to be due to the inhibition of degranulation. In one such example, it has been reported olopatadine inhibits IgE-mediated histamine release from human conjunctival mast cells (33). Thus, the histamine released by antigen-IgE stimulation could induce the production of TARC and MDC via H4R.

Because TARC levels in patients with AD correlate with the scoring of the AD index and eosinophil numbers (34, 35), an extracorporeal diagnostic agent, serum TARC (Shionogi & Co., Osaka, Japan), is used as a biomarker against AD in Japan. Our findings suggested that JNJ7777120 inhibited the infiltration of $CD4^+$ T cells in the skin lesions probably by inhibiting the production of TARC (Fig. 4), resulting in the alleviation of chronic dermatitis.

Prednisolone is used externally in the treatment of AD. In our model, prednisolone inhibited scratching count, dermatological score, the production of several cytokines, and the increase in serum IgE. Importantly, the combined treatment of olopatadine and JNJ7777120 could inhibit these parameters to almost similar extent. Glucocorticoids containing prednisolone frequently causes atrophy of skin and elicit side-effects by systemic administration. On the other hand, a new H4R antagonist from Palau Pharma is currently in Phase II clinical trial and has shown that the H4R antagonist is safe and very well tolerated. Therefore, our findings suggest the combined treatment of H1R and H4R antagonists might be a potent and safer therapeutic strategy to allergic diseases.

In conclusion, we clarified that histamine is involved in pruritus and the development of dermatitis in a model of chronic allergic dermatitis established in NC/Nga mice. In addition to the direct involvement of histamine in pruritus via H1R and H4R, we clarified that histamine was also associated with the regulation of Sema3A in keratinocytes and production of Th2 chemokines in BMMC, via H1R and H4R respectively. Thus, our findings indicated that combined treatment with a H1R antagonist plus H4R antagonist potentiated both anti-pruritic and anti-inflammatory effects, and had a pharmaceutical benefit equivalent to prednisolone. Our understanding of the roles of histamine in chronic dermatitis indicate that a blockade of the H4R antagonist as well as H1R antagonist might have more potential benefit for patients with AD.

Conflict of interest

The authors declare no financial or commercial conflict of interest.

References

1. Novak N, Bieber T, Leung DY. Immune mechanisms leading to atopic dermatitis. *J Allergy Clin Immunol* 2003; **112**:S128–S139.
2. Leung DY, Boguniewicz M, Howell MD, Nomura I, Hamid QA. New insights into atopic dermatitis. *J Clin Invest* 2004;**113**: 651–657.
3. Soumelis V, Reche PA, Kanzler H, Yuan W, Edward G, Homey B et al. Human epithelial cells trigger dendritic cell mediated allergic inflammation by producing TSLP. *Nat Immunol* 2002;**3**:673–680.
4. Repka-Ramirez MS, Baraniuk JN. Histamine in health and disease. *Clin Allergy Immunol* 2002;**17**:1–25.
5. Paus R, Schmelz M, Biro T, Steinhoff M. Frontiers in pruritus research: scratching the brain for more effective itch therapy. *J Clin Invest* 2006;**116**:1174–1185.
6. Heyer G, Dotzer M, Diepgen TL, Handwerker HO. Opiate and H1antagonist effects on histamine induced pruritus and allokinesis. *Pain* 1997;**73**:239–243.
7. Ikoma A, Rukwied R, Stander S, Steinhoff M, Miyachi Y, Schmelz M. Neuronal sensitization for histamine-induced itch in lesional skin of patients with atopic dermatitis. *Arch Dermatol* 2003;**139**:1455–1458.
8. Hofstra CL, Desai PJ, Thurmond RL, Fung-Leung WP. Histamine H4 receptor mediates chemotaxis and calcium mobilization of mast cells. *J Pharmacol Exp Ther* 2003;**305**: 1212–1221.
9. Ling P, Ngo K, Nguyen S, Thurmond RL, Edwards JP, Karlsson L et al. Histamine H4 receptor mediates eosinophil chemotaxis with cell shape change and adhesion molecule upregulation. *Br J Pharmacol* 2004;**142**: 161–171.
10. Gutzmer R, Diestel C, Mommert S, Kother B, Stark H, Wittmann M et al. Histamine H4 receptor stimulation suppresses IL-12p70 production and mediates chemotaxis in human monocyte-derived dendritic cells. *J Immunol* 2005;**174**:5224–5232.
11. Dunford PJ, O'Donnell N, Riley JP, Williams KN, Karlsson L, Thurmond RL. The histamine H4 receptor mediates allergic airway inflammation by regulating the activation of CD4+ T cells. *J Immunol* 2006;**176**:7062–7070.
12. Hirasawa N, Ohsawa Y, Katoh G, Shibata K, Ishihara K, Seyama T et al. Modification of the picryl chloride-induced allergic dermatitis model in mouse ear lobes by 12-O-tetradecanoylphorbol 13-acetate, and analysis of the role of histamine in the modified model. *Int Arch Allergy Immunol* 2009;**148**:279–288.
13. Cowden JM, Zhang M, Dunford PJ, Thurmond RL. The histamine H4 receptor mediates inflammation and pruritus in Th2-dependent dermal inflammation. *J Invest Dermatol* 2010;**130**:1023–1033.
14. Cowden JM, Riley JP, Ma JY, Thurmond RL, Dunford PJ. Histamine H4 receptor antagonism diminishes existing airway inflammation and dysfunction via modulation of Th2 cytokines. *Respir Res* 2010; **11**:86.
15. Takahashi Y, Kagawa Y, Izawa K, Ono R, Akagi M, Kamei C. Effect of histamine H4 receptor antagonist on allergic rhinitis in mice. *Int Immunopharmacol* 2009;**9**: 734–738.
16. Dunford PJ, Williams KN, Desai PJ, Karlsson L, McQueen D, Thurmond RL. Histamine H4 receptor antagonists are superior to traditional antihistamines in the attenuation of experimental pruritus. *J Allergy Clin Immunol* 2007;**119**: 176–183.
17. Rossbach K, Wendorff S, Sander K, Stark H, Gutzmer R, Werfel T et al. Histamine H4 receptor antagonism reduces hapten-induced scratching behaviour but not inflammation. *Exp Dermatol* 2009;**18**:57–63.
18. Seike M, Furuya K, Omura M, Hamada-Watanabe K, Matsushita A, Ohtsu H. Histamine H(4) receptor antagonist ameliorates chronic allergic contact dermatitis induced by repeated challenge. *Allergy* 2010;**65**:319–326.
19. Suwa E, Yamaura K, Oda M, Namiki T, Ueno K. Histamine H(4) receptor antagonist reduces dermal inflammation and pruritus in a hapten-induced experimental model. *Eur J Pharmacol* 2011;**667**:383–388.
20. Frosch PJ, Schwanitz HJ, Macher E. A double blind trial of H1 and H2 receptor antagonists in the treatment of atopic dermatitis. *Arch Dermatol Res* 1984;**276**: 36–40.
21. Tamura T, Amano T, Ohmori K, Manabe H. The effects of olopatadine hydrochloride on the number of scratching induced by repeated application of oxazolone in mice. *Eur J Pharmacol* 2005;**524**:149–154.
22. Ishii H, Sasaki Y, Ikemura T, Kitamura S, Ohmori K. Pharmacological studies on KW-4679, an antiallergic drug. (1): inhibitory effect on passive cutaneous anaphylaxis (PCA) and experimental asthma in rats and guinea pigs. *Nihon Yakurigaku Zasshi* 1995;**106**:289–298.
23. Greaves MW. Antihistamines in dermatology. *Skin Pharmacol Physiol* 2005;**18**: 220–229.
24. Herman SM, Vender RB. Antihistamines in the treatment of dermatitis. *J Cutan Med Surg* 2003;**7**:467–473.
25. Thurmond RL, Gelfand EW, Dunford PJ. The role of histamine H1 and H4 receptors in allergic inflammation: the search for new antihistamines. *Nat Rev Drug Discov* 2008;**7**:41–53.
26. Toyoda M, Nakamura M, Makino T, Hino T, Kagoura M, Morohashi M. Nerve growth factor and substance P are useful plasma markers of disease activity in atopic dermatitis. *Br J Dermatol* 2002;**147**:71–79.
27. Yamaguchi J, Aihara M, Kobayashi Y, Kambara T, Ikezawa Z. Quantitative analysis of nerve growth factor (NGF) in the atopic dermatitis and psoriasis horny layer and effect of treatment on NGF in atopic dermatitis. *J Dermatol Sci* 2009;**53**:48–54.
28. Kanda N, Watanabe S. Histamine enhances the production of nerve growth factor in human keratinocytes. *J Invest Dermatol* 2003;**121**:570–577.
29. Tominaga M, Ogawa H, Takamori K. Decreased production of semaphorin 3A in the lesional skin of atopic dermatitis. *Br J Dermatol* 2008;**158**:842–844.
30. Murota H, El-latif MA, Tamura T, Amano T, Katayama I. Olopatadine hydrochloride improves dermatitis score and inhibits scratch behavior in NC/Nga mice. *Int Arch Allergy Immunol* 2010;**153**:121–132.
31. Yamaura K, Oda M, Suwa E, Suzuki M, Sato H, Ueno K. Expression of histamine H4 receptor in human epidermal tissues and attenuation of experimental pruritus using H4 receptor antagonist. *J Toxicol Sci* 2009;**34**:427–431.
32. Harada D, Takada C, Nosaka Y, Takashima Y, Kobayashi K, Takaba K et al. Effect of orally administered KF66490, a phosphodiesterase 4 inhibitor, on dermatitis in mouse models. *Int Immunopharmacol* 2009;**9**:55–62.
33. Sharif NA, Xu SX, Miller ST, Gamache DA, Yanni JM. Characterization of the ocular antiallergic and antihistaminic effects of olopatadine (AL-4943A), a novel drug for treating ocular allergic diseases. *J Pharmacol Exp Ther* 1996;**278**:1252–1261.
34. Kakinuma T, Nakamura K, Wakugawa M, Mitsui H, Tada Y, Saeki H et al. Thymus and activation-regulated chemokine in atopic dermatitis: serum thymus and activation-regulated chemokine level is closely related with disease activity. *J Allergy Clin Immunol* 2001;**107**:535–541.
35. Morita E, Takahashi H, Niihara H, Dekio I, Sumikawa Y, Murakami Y et al. Stratum corneum TARC level is a new indicator of lesional skin inflammation in atopic dermatitis. *Allergy* 2010;**65**:1166–1172.

blood

2011 117: 3961-3967
Prepublished online February 16, 2011;
doi:10.1182/blood-2010-11-316794

Type of skin eruption is an independent prognostic indicator for adult T-cell leukemia/lymphoma

Yu Sawada, Ryosuke Hino, Kayo Hama, Shun Ohmori, Haruna Fueki, Shigenori Yamada, Shoko Fukamachi, Makiko Tajiri, Rieko Kubo, Manabu Yoshioka, Daiki Nakashima, Kazunari Sugita, Ryutaro Yoshiki, Takatoshi Shimauchi, Tomoko Mori, Kunio Izu, Miwa Kobayashi, Motonobu Nakamura and Yoshiki Tokura

Blood (print ISSN 0006-4971, online ISSN 1528-0020), is published weekly by the American Society of Hematology, 2021 L St, NW, Suite 900, Washington DC 20036.

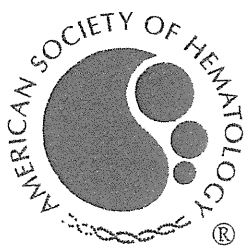

Type of skin eruption is an independent prognostic indicator for adult T-cell leukemia/lymphoma

Yu Sawada,[1] Ryosuke Hino,[1] Kayo Hama,[1] Shun Ohmori,[1] Haruna Fueki,[1] Shigenori Yamada,[1] Shoko Fukamachi,[1] Makiko Tajiri,[1] Rieko Kubo,[1] Manabu Yoshioka,[1] Daiki Nakashima,[1] Kazunari Sugita,[1] Ryutaro Yoshiki,[1] Takatoshi Shimauchi,[1] Tomoko Mori,[1] Kunio Izu,[2] Miwa Kobayashi,[1] Motonobu Nakamura,[1] and Yoshiki Tokura[1,3]

[1]Department of Dermatology, University of Occupational and Environmental Health, Kitakyushu, Fukuoka, Japan; [2]Department of Dermatology, Kyushu Kosei Nenkin Hospital, Kitakyushu, Fukuoka, Japan; and [3]Department of Dermatology, Hamamatsu University School of Medicine, Hamamatsu, Shizuoka, Japan

Cutaneous involvement is seen in ~ 50% of adult T-cell leukemia/lymphoma (ATLL) patients. We investigated the association between skin eruption type and prognosis in 119 ATLL patients. ATLL eruptions were categorized into patch (6.7%), plaque (26.9%), multipapular (19.3%), nodulotumoral (38.7%), erythrodermic (4.2%), and purpuric (4.2%) types. When the T stage of the tumor-node-metastasis-blood (TNMB) classification of mycosis fungoides/Sézary syndrome was applied to ATLL staging, 16.0% were T1, 17.7% T2, 38.7% T3, and 4.2% T4, and the remaining 23.5% were of the multipapular and purpuric types. For the patch type, the mean survival time (median survival time could not be estimated) was 188.4 months. The median survival times (in months) for the remaining types were as follows: plaque, 114.9; multipapular, 17.3; nodulotumoral, 17.3; erythrodermic, 3.0; and purpuric, 4.4. Kaplan-Meier curves of overall survival showed that the erythrodermic type had the poorest prognosis, followed by the nodulotumoral and multipapular types. The patch and plaque types were associated with better survival rates. Multivariate analysis demonstrated that the hazard ratios of the erythrodermic and nodulotumoral types were significantly higher than that of the patch type, and that the eruption type is an independent prognostic factor for ATLL. The overall survival was worse as the T stage became more advanced: the multipapular type and T2 were comparable, and the purpuric type had a significantly poorer prognosis than T1. (*Blood*. 2011;117(15): 3961-3967)

Introduction

Adult T-cell leukemia/lymphoma (ATLL) is a malignancy of mature $CD4^+$ T cells caused by the human T-cell lymphotropic virus type I (HTLV-1).[1-3] HTLV-1 infection is prevalent in southern Japan, especially in Kyushu,[4,5] and in the Caribbean region and Africa.[6,7] Based on the number of abnormal lymphocytes, organ involvement, and severity, ATLL is divided into 4 clinical categories: acute, lymphoma, chronic, and smoldering (Shimoyama classification).[8] This classification is the most common tool used for estimating the prognosis of ATLL patients. The smoldering type has the best prognosis, followed by the chronic type, lymphoma type, and acute type. The median survival times (MSTs) of the acute, lymphoma, and chronic types are 6.2, 10.2, and 24.3 months, respectively.[8] Thus, the acute and lymphoma types of ATLL are associated with remarkably poor prognoses despite advances in chemotherapy and allogeneic hematopoietic stem cell transplantation.[9-11] In contrast, the chronic and smoldering types are relatively indolent and can usually be managed with "watchful waiting" until the disease progresses to acute crisis, just as smoldering (asymptomatic) myeloma is managed.[12]

Studies have attempted to identify other prognostic factors for survival of ATLL patients. Advanced performance status, high blood lactate dehydrogenase (LDH) level, age of 40 years or more, more than 3 involved lesions, and hypercalcemia have all been associated with shortened survival.[13] The existence of hepatosplenomegaly and lymphadenopathy also indicates poor prognosis.[8,14] However, there has been no large study on the correlation between the type and spread of skin eruptions and the prognosis of ATLL.

Because cutaneous involvement can be recognized in approximately 50% of ATLL patients,[15,16] the evaluation of skin lesions in relation to prognosis is important. Tumor cells infiltrating the skin exhibit several differences in phenotype and function.[17,18] ATLL patients can develop various types of eruptions, including nodules, tumors, plaques, erythrodermas, and even purpuric lesions,[19,20] and the categorization of these eruption types remains unclear. In this study, we retrospectively analyzed the prognosis of ATLL on the basis of the skin manifestations. We classified the skin eruptions and applied the T stage of the tumor-node-metastasis-blood (TNMB) classification for mycosis fungoides (MF) and Sézary syndrome (SS) to the type of skin lesions of ATLL. Our results indicate that eruption type is a predictor for prognosis.

Methods

Patients

We analyzed 119 patients with newly diagnosed, untreated ATLL who had skin eruptions and were seen at the University of Occupational and Environmental Health and Kyushu Kosei Nenkin Hospital from April 1979 to December 2009. The cutoff date for analysis was June 2010. The diagnosis of ATLL was based on clinical features, histopathologically and cytologically proven mature T-cell malignancy, presence of anti–HTLV-1 antibody, and monoclonal integration of HTLV-1 proviral DNA into the blood and/or skin tumor cells, as described previously.[2,8,21,22] The subtypes

Submitted November 5, 2010; accepted January 28, 2011. Prepublished online as *Blood* First Edition paper, February 16, 2011; DOI 10.1182/blood-2010-11-316794.

The publication costs of this article were defrayed in part by page charge payment. Therefore, and solely to indicate this fact, this article is hereby marked "advertisement" in accordance with 18 USC section 1734.

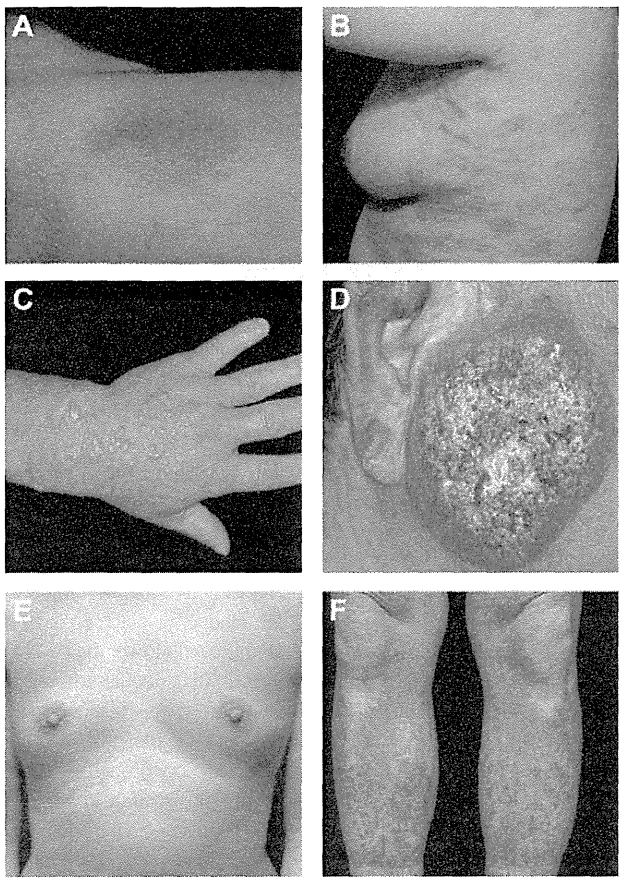

Figure 1. Clinical features of ATLL with skin eruptions. (A) Patch type, (B) plaque type, (C) multipapular type, (D) nodulotumoral type, (E) erythrodermic type, and (F) purpuric type.

of ATLL were classified according to the criteria established by the Lymphoma Study Group of Japan Clinical Oncology Group (Shimoyama classification).[8] Our retrospective, nonrandomized, observational study using existing data was granted an exemption from the institutional review board and was exempt from the requirement for written informed consent in accordance with the Declaration of Helsinki.

Clinical evaluation and definitions

The patients were categorized into 2 age groups: younger than 60 years and 60 years or older. Complications at diagnosis were classified into present and absent. Leukocytosis and lymphocytosis were defined as white blood cell count more than 12×10^9/L, and total lymphocyte count more than 6.5×10^9/L, respectively. LDH and calcium levels were classified into 2 groups according to a standard index.[13] We categorized skin eruptions of ATLL into 6 different types: patch, plaque, multipapular, nodulotumoral, erythrodermic, and purpuric (Figure 1). We defined the criteria for categorizing ATLL-related skin involvement into the patch type as no infiltrated erythema, the plaque type as infiltrated erythema, the multipapular type as multiple papules with diameter less than 1 cm, the nodulotumoral type as nodules or tumors with diameters more than 1 cm, the erythrodermic type as generalized erythema involving 80% or more of the patient's skin, and the purpuric type as red or purple discolorations that did not change with diascopy.

Statistical analyses

Overall survival (OS) was defined as the time from the date of first diagnosis to the date of death or the latest contact with the patient. Survival curves were drawn using the Kaplan-Meier method and were compared with the log-rank test. P values were calculated using the generalized Wilcoxon test. MST was defined as the time point at which the Kaplan-Meier survival curves crossed 50%. Mean survival time was provided when MST could not be calculated. To examine the multiple comparisons of the factors and of the pairs of groups, univariate and multivariate Cox regression analyses were applied to evaluate prognosis factors for survival. The effects of clinical parameters were evaluated as hazard ratios (HRs) and their 95% confidence intervals. All statistical analyses were performed using Dr SPSS II software (SPSS). A P value $< .05$ was considered statistically significant.

Results

Patient clinical characteristics

The clinical data of 119 patients with skin eruptions (ratio of male: female = 1.2:1) are summarized in Table 1. The mean age of the patients was 64.0 years (range, 23-91 years; SD, 12.00 years). According to Shimoyama classification, 40 (33.6%) patients were diagnosed with the acute type of ATLL, 6 (5.0%) with the chronic type, 17 (14.3%) with the lymphoma type, and 56 (47.1%) with the smoldering type. Twenty-three patients had complications at the time of diagnosis, including 7 patients with diabetes mellitus, 10 with hypertension, 3 with stroke, and 9 with opportunistic infections. Blood examination revealed that 36 patients (30.3%) had leukocytosis, 26 (21.9%) had lymphocytosis, and 49 (41.2%) had high LDH levels. Hypercalcemia was found in 70 patients (58.8%).

Patient skin lesions

We categorized the skin eruptions into the patch, plaque, multipapular, nodulotumoral, erythrodermic, and purpuric types (Figure 1). The most highly incident was the nodulotumoral type in 46 patients (38.7%), followed by the plaque type in 32 patients (26.9%), the multipapular type in 23 patients (19.3%), the patch type in 8 patients (6.7%), the erythrodermic type in 5 patients (4.2%), and the purpuric type in 5 patients (4.2%). Because the categorized skin eruptions of ATLL have similarities to those of MF/SS (with the exception of the multipapular and purpuric types), and because the TNMB classification for MF/SS[16] has been widely used, we attempted to apply the T stage of the TNMB classification to ATLL skin lesions. According to the MF/SS classification,[16] eruptions are classified into: T1 (patch/plaque, less than 10% of body surface), T2 (patch/plaque, more than 10% of body surface area), T3 (nodulotumoral type), and T4 (erythrodermic type). Ninety-one (76.5%) of our 119 patients could be classified using this system: 19 patients (16.0%) belonged to T1, 21 (17.7%) to T2, 46 (38.7%) to T3, and 5 (4.2%) to T4. The remaining 28 patients (23.5%) had multipapular (19.3%) and purpuric (4.2%) types, which are peculiar for ATLL and are not described in the T classification of MF/SS. We also evaluated these 2 types to investigate whether they are comparable with either the T1 or T4 category of the MF/SS classification system.

We examined the frequencies of the clinical subtypes of Shimoyama classification in each of the eruption types and T stages (Table 2). All patients with the erythrodermic type belonged to the acute type, whereas most of the patients with the patch type were grouped into the smoldering subtype. As the T stage advanced, the frequencies of the aggressive types (the acute and lymphoma types) increased, whereas those of the smoldering type decreased.

Survival by baseline clinical factors

Sixty-nine of our 119 patients died during the observation period, with a median follow-up duration of 3.0 years (range, 30 days-20.3 years). The MSTs of the acute, lymphoma, chronic, and

Table 1. Survival by baseline clinical factors

Factor	No. of evaluated cases	No. of deaths	MST, mos	*P*
Total	119	69		
Clinical subtype				< .001
Acute type	40	30	7.7	
Lymphoma type	17	12	15.0	
Chronic type	6	5	16.6	
Smoldering type	56	22	154.0	
Patient-related factors				
Sex				.956
Male	66	38	20.3	
Female	53	31	24.9	
Age, y				.702
≥ 60	81	46	24.5	
< 60	38	23	18.4	
Complications at diagnosis				.114
Absent	96	59	21.0	
Present				
Diabetes mellitus	7	3	14.8	
Hypertension	10	4	141.4*	
Stroke	3	2	17.2	
Opportunistic infections	9	4	49.3	
Hematologic factors				
WBC count, × 10^9/L				< .001
≥ 12.0	36	25	9.5	
< 12.0	83	44	47.8	
Total lymphocyte count, × 10^9/L				< .001
≥ 6.5	26	20	10.4	
< 6.5	93	49	47.8	
Laboratory factors				
LDH				< .001
≤ NI	70	37	47.9	
> NI	49	32	9.5	
Calcium				.420
≤ NI	49	28	27.8	
> NI	70	41	18.6	
Skin lesions				< .001
Patch type	8	2	188.4*	
Plaque type	32	9	114.9	
Multipapular type	23	12	17.3	
Nodulotumoral type	46	38	17.3	
Erythrodermic type	5	5	3.0	
Purpuric type	5	3	4.4	
T stage				< .001
T1	19	3	192.6*	
T2	21	8	47.9	
T3	46	38	17.3	
T4	5	5	3.0	

The cumulative probability of the survival rate was estimated using the Kaplan-Meier method and the *P* value was calculated using the generalized Wilcoxon test.

MST indicates median survival time; and NI, normal index.

*Mean survival time is given because the MST cannot be calculated.

smoldering types were 7.7, 15.0, 16.6, and 154.0 months, respectively (Table 1). Of the 69 fatal cases during the observation, 45 patients died of acute ATLL, 17 of acute crisis from the other subtypes, 5 of other diseases (3 of chronic pulmonary diseases and 2 of acute respiratory disease syndrome [ARDS]), and 2 patients of unknown causes.

The effects of various clinical factors on prognosis in the 119 patients were analyzed using the Kaplan-Meier method (Table 1). There was no statistically significant difference in survival rates between the absence and presence of any complication ($P = .114$), between the ≥ 60 years and < 60 years age groups ($P = .702$), or between males and females ($P = .956$). The survival rate was poor in patients with leukocytosis ($P < .001$), lymphocytosis ($P < .001$), and higher LDH levels ($P < .001$). Blood calcium level did not significantly affect survival in this study.

Survival and multivariate analyses in each eruption type

The MSTs were different between the types of skin eruptions. In the erythrodermic type, all 5 patients died of the disease with 3.0 months of MST. In the nodulotumoral type, the MST was 17.3 months, and 38 of 46 patients died, 17 of acute ATLL, 16 of acute crisis, 1 of ARDS, 2 of chronic pulmonary disease, and 2 of unknown causes. In the plaque type, the MST was 114.9 months, and 9 of 32 died of the disease. The multipapular type showed the same MST (17.3 months) as the nodulotumoral type, and 9 died of acute ATLL, 1 of acute crisis, 1 of ARDS, and 1 of chronic pulmonary disease. The patch type exhibited a good prognosis, with 188.4 months of mean survival time (the MST was not estimable). The purpuric type was found to have a poor prognosis, with an MST of 4.4 months and 3 of 5 patients dying of the disease.

Kaplan-Meier curves of the OS for each eruption type are shown in Figure 2A. The OS rate of the erythrodermic type was significantly lower than those of the other eruption types ($P < .001$, erythrodermic type vs the nodulotumoral, multipapular, plaque, or patch types). The OS rate of the nodulotumoral type was significantly lower than those of the multipapular, plaque, or patch types ($P = .010$, nodulotumoral type vs multipapular type; $P < .001$, nodulotumoral type vs plaque or patch type). The OS rate of the multipapular type was significantly lower than that of the patch type ($P = .045$). Therefore, the erythrodermic type of ATLL is associated with the poorest prognosis, followed by the nodulotumoral and multipapular types. The patch and plaque types showed better survival rates.

We performed univariate and multivariate analyses of the eruption types in a comparison with Shimoyama classification, sex, age, complications, leukocyte counts, lymphocyte counts, LDH level, and calcium level (Table 3). In the multivariate analysis, the smoldering type proved to be a good prognostic factor. We fixed the HR of the patch type to be 1, and then compared it with those of the other eruption types. In the univariate analysis, the HRs of the other eruption types were significantly higher than that of the patch type. In the multivariate analysis, the HRs of the nodulotumoral and erythrodermic types were significantly higher than that of the patch type. The purpuric type also showed such a tendency; however, this result provided limited power for tests against the other groups. The analysis demonstrated that the eruption type is an independent prognostic factor for ATLL.

Survival and univariate and multivariate analyses in each T stage

We also performed the univariate and multivariate analyses of T stage and other clinical and laboratory parameters for OS. Of 19 patients in the T1 stage, 3 died of the disease, and the mean survival time (the MST was not estimable) was 192.6 months (Table 1). In the T2 stage, 8 of 21 died of the disease and the MST was 47.9 months. In the T3 stage, the MST was 17.3 months and 38 of 46 patients died: 17 of acute ATLL, 16 of acute crisis, 1 of ARDS, 2 of chronic pulmonary disease, and 2 of unknown etiology. In the T4 stage, 5 patients died of the disease with 3.0 months of MST. The OS of the patients was worse as the T stage became more advanced (Figure 2B). Patients in the T1 stage had the longest OS, followed by patients in the T2-T4 stages ($P = .034$, T1 vs T2; $P < .001$, T1 vs T3 or T4; $P < .001$ T2 vs T3 or T4; and $P < .001$, T3 vs T4).

The multipapular and purpuric types are missing in the T stage of the MF/SS system due to their peculiarity. We therefore compared the OS of

Table 2. Frequencies of the clinical types of Shimoyama classification in each eruption type and T stage

	Acute type	Lymphoma type	Chronic type	Smoldering type	*P*
Eruption type					.015
Patch type	0	0	1 (12.8%)	7 (87.2%)	
Plaque type	9 (28.1%)	4 (12.5%)	0	19 (59.4%)	
Multipapular type	10 (43.5%)	2 (8.7%)	0	11 (47.8%)	
Nodulotumoral type	14 (30.4%)	10 (21.7%)	5 (10.9%)	17 (37.0%)	
Erythrodermic type	5 (100%)	0	0	0	
Purpuric type	2 (40.0%)	1 (20.0%)	0	2 (40.0%)	
T stage					.004
T1	2 (10.5%)	1 (5.3%)	0	16 (84.2%)	
T2	7 (33.3%)	3 (14.3%)	1 (4.8%)	10 (47.6%)	
T3	14 (30.4%)	10 (21.7%)	5 (10.9%)	17 (37.0%)	
T4	5 (100%)	0	0	0	

these 2 eruption types with those of the T stages. Patients with the multipapular type and T2 had a similar outcome (Figure 2C), and there was no statistical significance ($P = .415$). Patients with the purpuric type had a significantly poorer prognosis than those with T1 ($P = .001$); Figure 2D). The differences in OS between the purpuric type and the other T stages were not statistically significant ($P = .412$, purpuric type vs T2; $P = .257$; purpuric type vs T3; $P = .099$, purpuric type vs T4).

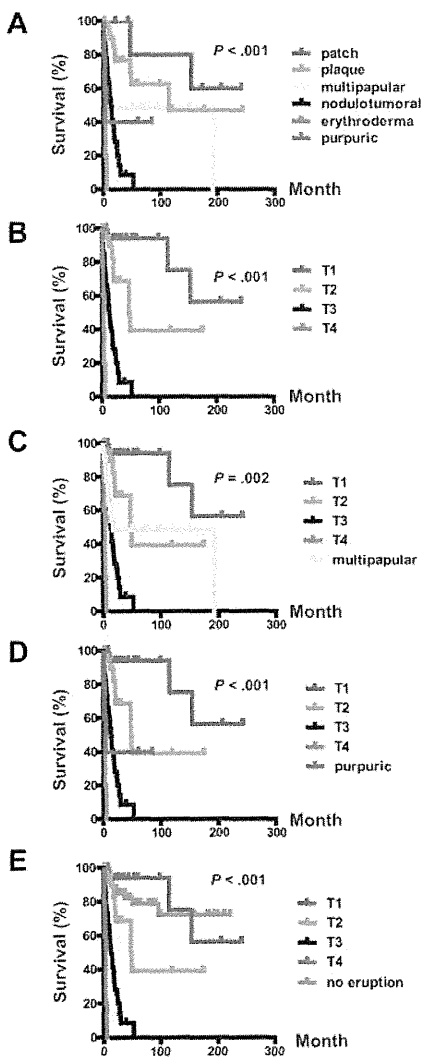

Figure 2. OS of ATLL patients with skin eruptions. (A) OS rates of skin eruption types. (B) OS rate of T stage. (C) OS rate of the T stage and the multipapular type. (D) OS rate of the T stage and the purpuric type. (E) OS rate of the T stage and the no-eruption type.

We performed univariate and multivariate analyses of T stage and clinical and laboratory parameters with the HR of T1 set as 1 (Table 3). The univariate analysis revealed that the prognoses of T2, T3, T4, and the multipapular and purpuric types were significantly higher than that of T1. In the multivariate analysis, the HR of T3 and T4 and the multipapular and purpuric types were significantly higher than that of T1.

Survival and univariate and multivariate analyses in each T stage and in the no-eruption group

We performed univariate and multivariate analyses of T stage by comparing them with the no-eruption group and other clinical and laboratory parameters for OS. Of 51 patients without skin eruptions, 10 died of the disease and the mean survival time (the MST was not estimable) was 66.5 months. When classifying the no-eruption patients into each clinical Shimoyama subtype, 7 patients (13.7%) belonged to the acute type, 5 (9.8%) to the lymphoma type, 12 (23.5%) to the chronic type, and 27 (52.9%) to the smoldering type. The OS of the patients without eruption was better than those at T2-T4 (Figure 2E; no-eruption group vs T2, $P = .033$; no eruption group vs T3 or T4, $P < .001$). There was no statistically significant difference in OS between the no-eruption group and T1.

We performed univariate and multivariate analyses of T stage, including the no-eruption group and clinical and laboratory parameters, by assigning a value of 1 to the HR of T1 (Tables 4 and 5). The univariate and multivariate analyses revealed that the prognoses of T3 and T4 were significantly worse than that of T1.

Discussion

In the present study, we investigated the association of each type of skin eruption with prognosis in ATLL patients and attempted to apply the T stage of MF/SS classification to the assessment of ATLL skin lesions. We classified ATLL skin eruptions into 6 categories: patch, plaque, multipapular, nodulotumoral, erythrodermic, and purpuric. Table 2 shows that the frequencies of the clinical subtypes of Shimoyama classification were different for each eruption type and T stage. All erythrodermic patients belonged to the acute type, whereas most of patients with the patch type were of the smoldering type. This raised the possibility that prognosis is different among the individual eruption types. Our results revealed the poorest prognosis in the erythrodermic type, followed by the nodulotumoral and multipapular types. The patch and plaque types exhibited better survival rates. Moreover, our multivariate analysis demonstrated that the HRs of the erythrodermic and nodulotumoral

Table 3. Cox analysis of eruption type and T stage for clinical factors and OS

	Univariate		Multivariate (eruption type and clinical factors)		Multivariate (T stage and clinical factors)	
Clinical factor	**HR (95% CI)**	***P***	**HR (95% CI)**	***P***	**HR (95% CI)**	***P***
Clinical subtype						
Acute type	1		1		1	
Lymphoma type	0.5 (0.1-0.8)	.013	0.9 (0.3-2.5)	.852	0.9 (0.1-1.3))	.852
Chronic type	0.1 (0.3-1.1)	.082	0.4 (0.1-1.4)	.167	0.4 (0.3-2.4)	.140
Smoldering type	0.1 (0.1-0.2)	< .001	0.2 (0.8-0.6)	.002	0.2 (0.1-0.6)	.003
Patient-related factors						
Sex						
Male	1		1		1	
Female	1.0 (0.6-1.6)	.903	1.2 (0.7-2.1)	.576	1.2 (0.7-2.1)	.576
Age, y						
< 60	1		1		1	
≥ 60	1.0 (0.6-1.7)	.922	0.9 (0.5-1.6)	.658	0.9 (0.5-1.5)	.578
Complications at diagnosis						
Absent	1		1		1	
Present						
Diabetes mellitus	0.6 (0.2-2.0)	.427	0.5 (0.1-1.9)	.314	0.5 (0.1-1.8)	.274
Hypertension	0.4 (0.2-1.2)	.119	1.0 (0.3-3.9)	.958	1.1 (0.3-4.2)	.905
Stroke	1.8 (0.4-7.3)	.425	3.5 (0.6-19.4)	.161	2.9 (0.5-17.3)	.256
Opportunistic infection	1.0 (0.4-2.6)	.927	1.0 (0.3-3.1)	.958	1.1 (0.3-3.4)	.938
Hematologic factors						
WBC count, × 10^9/L						
< 12.0	1		1		1	
≥ 12.0	3.6 (2.1-6.2)	< .001	1.8 (0.6-5.2)	.279	1.7 (0.6-4.9)	.325
Total lymphocyte count, × 10^9/L						
< 6.5	1		1		1	
≥ 6.5	3.7 (2.0-6.5)	< .001	1.1 (0.5-2.6)	.803	1.1 (0.5-2.7)	.768
Laboratory factors						
LDH						
≤ NI	1		1		1	
> NI	3.0 (1.8-4.9)	< .001	1.2 (0.6-2.2)	.581	1.2 (0.6-2.2)	.599
Calcium						
≤ NI	1		1		1	
> NI	1.3 (0.8-2.1)	.381	1.0 (0.6-1.8)	.960	1.0 (0.6-1.8)	.914
Eruption type						
Patch	1		1			
Plaque	2.2 (0.5-10.9)	.321	1.4 (0.3-8.0)	.680		
Nodulotumoral	12.5 (2.7-57.1)	.001	8.8 (1.6-48.0)	.012		
Erythrodermic	68.4 (11.5-405.9)	< .001	21.2 (3.0-150.3)	.002		
Multipapular	4.8 (1.0-22.6)	.045	3.5 (0.6-20.1)	.159		
Purpuric	7.1 (1.1-45.7)	.039	6.8 (0.9-53.7)	.071		
T stage						
T1	1				1	
T2	4.0 (1.0-15.1)	.047			2.2 (0.5-9.8)	.304
T3	15.3 (4.4-52.8)	< .001			11.3 (2.8-46.0)	.001
T4	83.9 (17.8-394.6)	< .001			27.5 (5.0-151.8)	< .001
Multipapular type	5.8 (1.6-20.9)	.007			8.1 (1.4-47.1)	.045
Purpuric type	8.6 (1.7-44.5)	.010			8.1 (1.4-47.1)	.020

CI indicates confidence interval; and NI, normal index.

types were significantly higher than that of the patch type, and that skin eruption is an independent prognostic factor for ATLL.

Table 4. Univariate analyses of T stage compared with patients having no skin eruptions

	Univariate	
Clinical factor	**HR (95% CI)**	***P***
T stage		
T1	1	
T2	3.6 (0.9-13.6)	.059
T3	16.4 (4.9-55.1)	< .001
T4	127.4 (26.2-618.1)	< .001
No eruption	1.3 (0.3-4.8)	.670

It has been reported that the smoldering type of ATLL with skin eruptions, especially those of the nodulotumoral type, has a poorer prognosis than ATTL without skin involvement.[19] Another group of investigators reported that the MSTs of the nodulotumoral and maculopapular types were 26 and 80 months, respectively, which are significantly shorter than those in ATLL without cutaneous eruptions.[23] Our findings are in agreement with these observations, and further clarify the relationship between type of skin lesion and prognosis. Skin-targeted therapy using topical steroids, psoralen photochemotherapy, or narrow-band UVB therapy[19] may improve the prognosis of ATLL for patients with skin eruptions.

The purpuric type of ATLL is one of the rarest skin eruptions of ATLL,[24] and has been reported to occur in 1.6% of ATLL patients with

Table 5. Cox multivariate analyses of clinical factors and OS compared with patients having no eruption

	Multivariate	
Clinical factor	**HR (95% CI)**	***P***
Clinical subtype		
Acute type	1	
Lymphoma type	2.4 (0.8-7.2)	.110
Chronic type	0.3 (0.1-0.9)	.036
Smoldering type	0.4 (0.1-1.1)	.068
Patient-related factors		
Sex		
Male	1	
Female	0.8 (0.4-1.4)	.440
Age, y		
< 60	1	
≥ 60	0.4 (0.2-0.8)	.012
Complications at diagnosis		
Absence	1	
Presence		
Diabetes *mellitus*	1.9 (0.7-4.8)	.188
Hypertension	0.6 (0.2-2.1)	.443
Stroke	2.6 (0.6-10.5)	.191
Opportunistic infection	1.1 (0.2-6.1)	.925
Hematologic factors		
WBC count, × 10^9/L		
< 12.0	1	
≥ 12.0	1.1 (0.3-3.5)	.864
Total lymphocyte count, × 10^9/L		
< 6.5	1	
≥ 6.5	2.0 (0.7-5.9)	.197
Laboratory factors		
LDH		
≤ NI	1	
> NI	1.2 (0.7-2.1)	.596
Calcium		
≤ NI	1	
> NI	1.1 (0.6-1.9)	.826
T stage		
T1	1	
T2	2.4 (0.6-9.7)	.227
T3	13.4 (3.3-53.9)	< .001
T4	60.8 (10.1-366.4)	< .001
No eruption	0.9 (0.2-3.6)	.847

CI indicates confidence interval; and NI, normal index.

skin lesions.[19] However, its incidence is higher than was previously thought, because we documented a 4.2% frequency in this study. The production of granzyme B by ATLL cells may lead to the destruction of vessels and the development of purpuric eruptions in these patients.[24] The prognosis for the purpuric type of skin lesion has not been investigated because of the rarity of this type. There have been 9 cases of the purpuric type reported in the literature.[24-31] When these are divided into the punctate and macular subtypes, the prognosis of the punctate purpuric subtype might be better than the macular purpuric subtype.[24-31] In our 5 purpuric cases, 2 cases of the punctuate purpuric subtype survived, with a 73.4-month mean survival time (the MST was not estimable), whereas 3 cases of the macular purpuric subtype died with 2.1 months of the MST. This suggests that the punctuate subtype has a good clinical prognosis, and the poor prognosis of the total purpuric type is derived from the macular subtype.

In addition to the purpuric type, the erythrodermic type is a rare skin manifestation in ATLL patients, with a prevalence of 3.5% reported in a previous study[19] and 4.2% in the present study. The majority of ATLL cases associated with the erythrodermic type of skin lesion are aggressive. In our study, all patients with erythrodermic lesions also belonged to the acute type and had the poorest prognosis among all skin eruption types. In patients with cutaneous T-cell lymphoma (CTCL), the erythrodermic type is typically termed SS and also has a poor prognosis.[16] In some erythrodermic CTCL patients, the decreased expression of intercellular adhesion molecule-1 by keratinocytes may lead to an inability of malignant T cells to enter the epidermis and infiltrate the blood and other organs.[32] This pathomechanism in erythrodermic CTCL can also be applied to ATLL, resulting in poor prognosis. Skin biopsy specimens of the erythrodermic type of ATLL revealed scant tumor cell infiltration into the epidermis.[33,34]

We applied MF/SS classification T stages to ATLL assessment, and demonstrated that the OS was worse as the T stage became more advanced. The results shown in Table 3 indicated that the prognosis of T1 stage was better than that for T2, suggesting that the difference in the body surface area of skin lesions is associated with the prognosis of ATLL. Moreover, the prognosis of T3 patients was poorer than those of T1 and T2, indicating that the depth of tumor-cell infiltration is associated with survival rate. T-stage classification accurately reflects the prognosis of ATLL and MF/SS. However, the multipapular and purpuric types are not applicable to T stage. We found that the multipapular type and T2 had similar outcomes, and that the purpuric type had a significantly poorer prognosis than T1. This may provide clinically useful information for patient management and choice of therapy. Moreover, our present study demonstrated that skin eruption is an independent prognostic factor for ATLL patients: the presence of skin eruptions may indicate poorer outcome compared with no eruptions. Therefore, evaluation of skin lesions and treatments targeting the skin may be important for improving clinical outcome.

Acknowledgments

We thank R. Ide (Department of Work Systems and Health, Institute of Industrial Ecological Sciences, University of Occupational and Environmental Health) and Y. Miyamura (Department of Environmental Epidemiology, University of Occupational and Environmental Health) for advising on the statistical analyses.

This work was supported by Grants-in-Aid for Science Research from the Ministry of Education, Science, Sports, and Culture of Japan.

Authorship

Contribution: Y.S. collected and analyzed the data and wrote the manuscript; R.H. analyzed the data; K.H. collected the data; S.O., H.F., S.Y., S.F., M.T., R.K., M.Y., D.N., K.S., R.Y., T.S., T.M., K.I., M.K., and M.N. diagnosed and treated ATLL patients; and Y.T. organized the study.

Conflict-of-interest disclosure: The authors declare no competing financial interests.

Correspondence: Yu Sawada, MD, Department of Dermatology, University of Occupational and Environmental Health, 1-1 Iseigaoka, Yahatanishi-ku, Kitakyushu 807-8555, Japan; e-mail: longago@med.uoeh-u.ac.jp; or Ryosuke Hino, MD, PhD, Department of Dermatology, University of Occupational and Environmental Health, 1-1 Iseigaoka, Yahatanishi-ku, Kitakyushu 807-8555, Japan; e-mail: hinoti@med.uoeh-u.ac.jp.

References

1. Uchiyama T, Yodoi J, Sagawa K, et al. Adult T-cell leukemia: clinical and hematologic features of 16 cases. *Blood.* 1977;50(3):481-492.
2. Yoshida M, Miyoshi I, Hinuma Y. Isolation and characterization of retrovirus from cell lines of human adult T-cell leukemia and its implication in the disease. *Proc Natl Acad Sci U S A.* 1982; 79(6):2031-2035.
3. Tsukasaki K, Hermine O, Bazarbachi A, et al. Definition, prognostic factors, treatment, and response criteria of adult T-cell leukemia-lymphoma: a proposal from an international consensus meeting. *J Clin Oncol.* 2009;27(3):453-459.
4. Iwanaga M, Chiyoda S, Kusaba E, Kamihira S. Trends in the seroprevalence of HTLV-1 in Japanese blood donors in Nagasaki Prefecture, 2000-2006. *Int J Hematol.* 2009;90(2):186-190.
5. Tajima K. The 4th nation-wide study of adult T-cell leukemia/lymphoma (ATL) in Japan: estimates of risk of ATL and its geographical and clinical features. The T- and B-cell Malignancy Study Group. *Int J Cancer.* 1990;45(2):237-243.
6. Levine PH, Blattner WA, Clark J, et al. Geographic distribution of HTLV-I and identification of a new high-risk population. *Int J Cancer.* 1988; 42(1):7-12.
7. Fleming AF, Maharajan R, Abraham M, at al. Antibodies to HTLV-I in Nigerian blood-donors, their relatives and patients with leukaemias, lymphomas and other diseases. *Int J Cancer.* 1986; 38(6):809-813.
8. Shimoyama M. Diagnosis criteria and classification of clinical subtypes of adult T-cell leukemia-lymphoma: a report from the Lymphoma Study Group. *Br J Hematol.* 1991;79(3):428-437.
9. Yamada Y, Tomonaga M, Fukuda H, et al. A new G-CSF-supported combination chemotherapy, LGS15, for adult T-cell leukemia-lymphoma: Japan Clinical Oncology Group Study 9303. *Br J Haematol.* 2001;113(2):375-382.
10. Fukushima T, Miyazaki Y, Honda S, et al. Allogenic hematopoietic stem cell transplantation provides sustained long-term survival for patients with adult T-cell leukemia/lymphoma. *Leukemia.* 2005;19(5):829-834.
11. Tsukasaki K, Utsunomiya A, Fukuda H, et al. VCAP-AMP-VECP compared with biweekly CHOP for adult T-cell leukemia-lymphoma: Japan clinical oncology group study JCOG 9801. *J Clin Oncol.* 2007;25:5458-5464.
12. Bladé J, Dimopoulos M, Rosiñol L, Rajkumar SV, Kyle RA. Smoldering (asymptomatic) multiple myeloma: current diagnostic criteria, new predictors of outcome, and follow-up recommendations. *J Clin Oncol.* 2010;28(4):690-697.
13. Lymphoma Study Group. Major prognostic factors of patients with adult T-cell leukemia-lymphoma: a cooperative study. Lymphoma Study Group (1984-1987). *Leuk Res.* 1991;15(2-3):81-90.
14. Broder S. NIH conference: T-cell lymphoproliferative syndrome associated with human T-cell leukemia/lymphoma virus. *Ann Intern Med.* 1984; 100(4):543-557.
15. Yamaguchi T, Ohshima K, Karube K, et al. Clinicopathological features of cutaneous lesions of adult T-cell leukaemia/lymphoma. *Br J Dermatol.* 2005;152(1):76-81.
16. Willemze R, Jaffe ES, Burg G, et al. WHO-EORTC classification for cutaneous lymphomas. *Blood.* 2005;105(10):3768-3785.
17. Shimauchi T, Imai S, Hino R, Tokura Y. Production of thymus and activation-regulated chemokine and macrophage-derived chemokine by CCR4+ adult T-cell leukemia cells. *Clin Cancer Res.* 2005;11(6):2427-2435.
18. Shimauchi T, Kabashima K, Nakashima D, et al. Augmented expression of programmed death-1 in both neoplastic and non-neoplastic CD4+ T-cells in adult T-cell leukemia/lymphoma. *Int J Cancer.* 2007;121(12):2585-2590.
19. Setoyama M, Katahira Y, Kanzaki T. Clinicopathologic analysis of 124 cases of adult T-cell leukemia/lymphoma with cutaneous manifestations: the smouldering type with skin manifestations has a poorer prognosis than previously thought. *J Dermatol.* 1999;26(12):785-790.
20. Chan HL, Su IJ, Kuo T, et al. Cutaneous manifestations of adult T-cell leukemia/lymphoma. Report of three different forms. *J Am Acad Dermatol.* 1985;13(2, pt 1):213-219.
21. Yamada Y. Phenotypic and function analysis of leukemic cells from 16 patients with adult T-cell leukemia/lymphoma. *Blood.* 1983;61(1):192-199.
22. Tsukasaki K, Ikeda S, Murata K, et al. Characteristics of chemotherapy-induced clinical remission in long survivors with aggressive adult T-cell leukemia/lymphoma. *Leuk Res.* 1993;17(2):157-166.
23. Yamaguchi T, Nakayama J. Clinicopathological features of cutaneous lesions of adult T-cell leukemia/lymphoma [Article in Japanese]. *Skin Cancer.* 2006;21(3):268-272.
24. Shimauchi T, Hirokawa Y, Tokura Y. Purpuric adult T-cell leukaemia/lymphoma: expansion of unusual CD4/CD8 double-negative malignant T cells expressing CCR4 but bearing the cytotoxic molecule granzyme B. *Br J Dermatol.* 2005; 152(2):350-352.
25. Adachi A, Kunisada M, Yamada T, et al. Two cases of adult T cell leukemia/lymphoma with petechiae as the first symptom [Article in Japanese]. *Japanese Journal of Clinical Dermatology (Rinsho Hifuka)* 2003;45(3):361-364.
26. Masada M, Nakashima K, Shibazaki Y, et al. Adult T cell leukemia in which petechiae are the only skin manifestation [Article in Japanese]. Clinical Dermatology (Hifuka no Rinsho). 1999;41(8): 1379-1381.
27. Katahira Y, Setoyama M, Tashiro M. Adult T-cell leukemia with purpura [Article in Japanese]. *Practical Dermatology (Hifubyo Shinryo).* 1992;14(3): 255-258.
28. Fukaya T, Yamanaka K, Sato H, et al. A case of various skin manifestations of ATL [Article in Japanese]. *Lymphomas of the Skin (Hifu no Lymphoma).* 1989;8:30-33.
29. Okada J, Imafuku S, Tsujita J, et al. Case of adult T-cell leukemia/lymphoma manifesting marked purpura. *J Dermatol.* 2007;34(11):782-785.
30. Mizutani K, Umezawa Y, Ohta Y, et al. Adult T-cell leukemia with purpura [Article in Japanese]. *Clinical Dermatology (Hifuka no Rinsho).* 2007;49(6): 683-686.
31. Tabata R, Tabata C, Namiuchi S, et al. Adult T-cell lymphoma mimicking Henoch-Schönlein purpura. *Mod Rheumatol.* 2007;17(1):57-62.
32. Nickoloff BJ, Griffiths CE, Baadsgaard O, et al. Markedly diminished epidermal keratinocyte expression of intercellular adhesion molecule-1 (ICAM-1) in Sézary syndrome. *JAMA.* 1989; 261(15):2217-2221.
33. Hashizume H, Nakayama F, Oku T, Takigawa M. Adult T-cell leukemia with regression of erythroderma and simultaneous emergence of leukemia. *J Am Acad Dermatol.* 1992;27(5, pt 2):846-849.
34. Nagatani T, Miyazawa M, Matsuzaki T, et al. Successful treatment of adult T-cell leukemia/lymphoma with MACOP-B, M-FEPA and VEPP-B combination chemotherapy. *J Dermatol.* 1993; 20(10):623-629.

Activated regulatory T cells are the major T cell type emigrating from the skin during a cutaneous immune response in mice

Michio Tomura,[1] Tetsuya Honda,[2] Hideaki Tanizaki,[2] Atsushi Otsuka,[2] Gyohei Egawa,[2,3] Yoshiki Tokura,[4] Herman Waldmann,[5] Shohei Hori,[6] Jason G. Cyster,[7] Takeshi Watanabe,[3] Yoshiki Miyachi,[2] Osami Kanagawa,[1] and Kenji Kabashima[2,3]

[1]Laboratory for Autoimmune Regulation, Research Center for Allergy and Immunology, RIKEN, Yokohama City, Japan. [2]Department of Dermatology and [3]Center for Innovation in Immunoregulative Technology and Therapeutics, Kyoto University Graduate School of Medicine, Japan. [4]Department of Dermatology, University of Occupational and Environmental Health, Kitakyushu, Japan. [5]Sir William Dunn School of Pathology, Oxford, United Kingdom. [6]Research Unit for Immune Homeostasis, Research Center for Allergy and Immunology, RIKEN. [7]Howard Hughes Medical Institute and Department of Microbiology and Immunology, UCSF, San Francisco, California.

Tregs play an important role in protecting the skin from autoimmune attack. However, the extent of Treg trafficking between the skin and draining lymph nodes (DLNs) is unknown. We set out to investigate this using mice engineered to express the photoconvertible fluorescence protein Kaede, which changes from green to red when exposed to violet light. By exposing the skin of Kaede-transgenic mice to violet light, we were able to label T cells in the periphery under physiological conditions with Kaede-red and demonstrated that both memory phenotype $CD4^+Foxp3^-$ non-Tregs and $CD4^+Foxp3^+$ Tregs migrated from the skin to DLNs in the steady state. During cutaneous immune responses, Tregs constituted the major emigrants and inhibited immune responses more robustly than did LN-resident Tregs. We consistently observed that cutaneous immune responses were prolonged by depletion of endogenous Tregs in vivo. In addition, the circulating Tregs specifically included activated $CD25^{hi}$ Tregs that demonstrated a strong inhibitory function. Together, our results suggest that Tregs in circulation infiltrate the periphery, traffic to DLNs, and then recirculate back to the skin, contributing to the downregulation of cutaneous immune responses.

Introduction

Lymphocytes travel throughout the body to conduct immune surveillance. $CD4^+$ helper T cells are central organizers in immune responses. Upon stimulation, naive $CD4^+$ T cells differentiate into effector Th cells (1). $Foxp3^+$ Tregs represent a unique subpopulation of $CD4^+$ T cells that are important for maintenance of immunological homeostasis and self tolerance (2, 3). Naive T cells circulate between blood and secondary lymphoid tissues (4–7). However, it is debatable whether T cells travel through uninflamed peripheral tissues as part of their recirculation route. One type of peripheral tissue with the active afferent limb of the lymphatic system is, for example, the skin, and memory/effector T cells migrate to inflamed skin using CCR4 and CCR10 (8–10). Classic studies employing cannulation of afferent lymph vessels have shown that $CD4^+$ memory/effector cells make up nearly all cells in the afferent lymph of sheep (6, 11–13). On the other hand, Debes et al. have reported that $CD4^+$ cells, especially naive subsets, migrate from the skin in a CCR7-dependent manner using subcutaneous injection of fluorescent-labeled lymphocytes (14). However, the above experiments require traumatic or artificial procedures to follow or label T cells. Therefore, it is of interest to clarify whether T cells in the peripheral organs such as the skin migrate to draining LNs (DLNs) and to identify the T cell subsets of migration and their roles under physiological conditions.

To directly assess cells migrating from the peripheral tissue, we have devised a new experimental system that involves labeling resident cells using Tg mice expressing the Kaede protein. Kaede is a photoconvertible green fluorescence protein cloned from stony coral (15, 16) that changes its color from green to red when exposed to violet light (16). Therefore, the Kaede-Tg mouse system is an ideal tool for monitoring precise cellular movements in vivo at different stages of the immune response (17).

Here, we used the skin as a representative of the peripheral organs and observed the movement of cells from the skin using Kaede-Tg mice (17). A high proportion of the migrating cells into the DLNs were Tregs that had a stronger capacity to suppress acquired immune responses than LN-resident Tregs. Moreover, these migrating T cells recirculated into the skin upon elicitation to terminate immune responses.

Results

Detection of cell migration from the skin in the steady state using Kaede-Tg mice. To monitor cell migration from the skin in vivo, the abdominal skin of Kaede-Tg mice was photoconverted by exposure to violet light for 10 minutes (see Methods). Before photoconversion, all the cells in the skin of Kaede-Tg mice expressed only Kaede-green fluorescence (Kaede-green) (Figure 1, A and B). Immediately after violet light exposure to the skin, the whole skin tissue (Supplemental Figure 1; supplemental material available online with this article; doi:10.1172/JCI40926DS1) and the skin cells of the photoconverted area showed red signal (Kaede-red), whereas virtually no draining axillary LN cells (Figure 1, A and B, and Supplemental Figure 2) or blood cells (Supplemental Figure 2)

Authorship note: Michio Tomura and Tetsuya Honda contributed equally to this work.

Conflict of interest: The authors have declared that no conflict of interest exists.

Citation for this article: *J Clin Invest.* 2010;120(3):883–893. doi:10.1172/JCI40926.

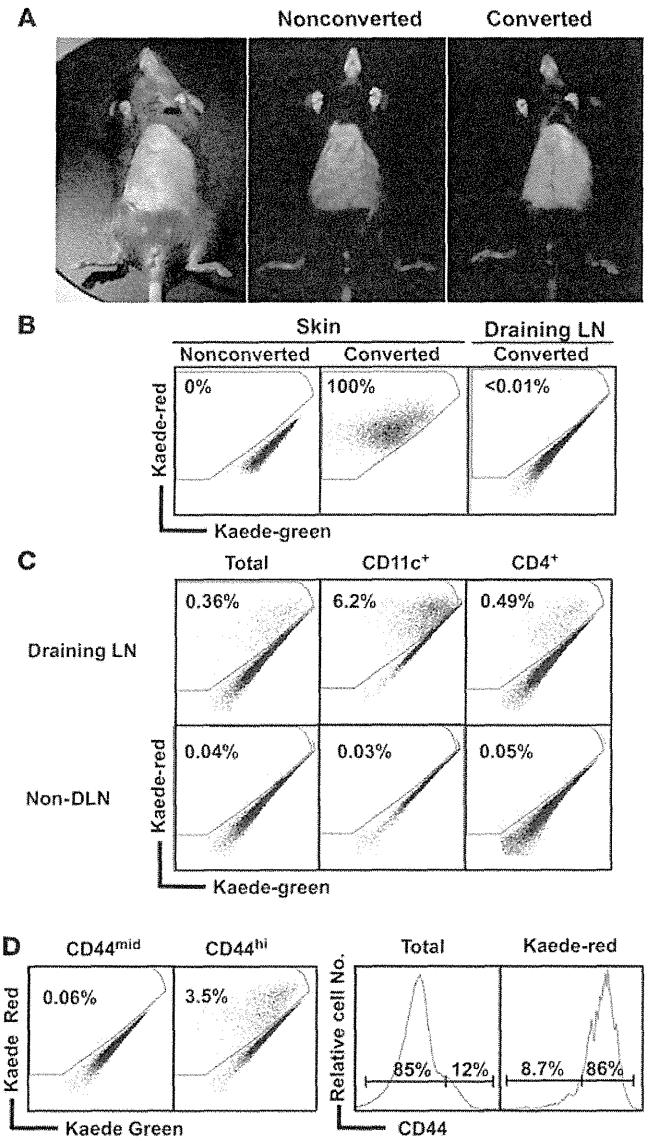

Figure 1

Cell migration from the skin to the DLN in the steady state. (**A**) Kaede-Tg mice were photoconverted on the clipped abdominal skin as described in Methods and observed with a fluorescence stereoscopic microscope. Nonphotoconverted clipped skin is shown as a control (middle). Note: nonclipped area remains black since light cannot reach. (**B**) Skin and draining axillary LN cells resected immediately after violet light exposure of the abdominal skin and resected skin cells not exposed to violet light were subjected to flow cytometric analysis to evaluate the photoconversion. (**C** and **D**) Twenty-four hours after photoconversion of the abdominal skin, cells from the draining axillary and other nondraining cervical and popliteal peripheral LNs were stained with CD11c and CD4 mAbs (**C**) and CD4 and CD44 mAbs (**D**) and subjected to flow cytometry. These data are representative of at least 5 experiments. Numbers within plots or histograms (**B**–**D**) indicate percentage of cells in the respective areas.

were photoconverted. Although we found that Kaede-red proteins could be detected in the extracellular fluids when incubated for 24 hours after photoconversion of the LN cells (Supplemental Figure 3), we confirmed that the extracellular photoconverted Kaede proteins could not be transferred into T cells in vitro (Supplemental Figure 4).

To evaluate cell migration from the skin in the steady state, the clipped abdominal skin of Kaede-Tg mice was exposed to violet light as in Figure 1A, and 24 hours later, the draining axillary and nondraining cervical and popliteal LN cells were subjected to flow cytometry. We found that 0.36% of the DLN cells showed the Kaede-red phenotype (Figure 1C), suggesting a fraction of cells in the skin migrate to the DLNs. It is generally thought that dendritic cells are the major migrants from the skin in the steady state, and in fact 6.2% of $CD11c^+$ dendritic cells were of the Kaede-red phenotype in the DLNs (Figure 1C). In contrast, almost no Kaede-red $CD11c^+$ dendritic cells were detected in the non-DLNs (Figure 1C). We next evaluated $CD4^+$ T cell migration from the skin and found that 0.49% of $CD3^+CD4^+$ T cells in the DLNs had the Kaede-red phenotype (Figure 1C). Although the frequencies of the Kaede-red positivity among dendritic cells and $CD3^+CD4^+$ T cells differed, the absolute numbers of Kaede-red dendritic cells and $CD4^+$ T cells were comparable ($CD4^+$ T cells vs. $CD11c^+$ dendritic cells: 11621 ± 2716 cells per LN vs. 9063 ± 2333 cells per LN, n = 5 each, average ± SD). Moreover, the ratio of Kaede-red cells was higher in $CD44^{hi}$ memory T cells than in $CD44^{mid}$ naive T cells (Figure 1D). Consistently, the majority of Kaede-red migratory cells were of the $CD44^{hi}$ memory phenotype (Figure 1D). These results suggest that predominantly T cells with the memory surface phenotype migrate from the skin into DLNs, even in the steady state.

Migration of Tregs from the skin to the DLNs. Immune responses and homeostasis are regulated by the functions of memory/effector T cells and Tregs. To determine the behaviors of these populations, we intercrossed Kaede-Tg mice with Foxp3 reporter mice expressing human CD2 and human CD52 chimeric protein, which are designated as Kaede/$Foxp3^{hCD2/hCD52}$ mice. Since $Foxp3^+$ cells coexpress hCD2 on the cell surface, live $Foxp3^+$ Tregs could be labeled and sorted with anti-hCD2 monoclonal Ab. The DLN cells from Kaede/$Foxp3^{hCD2/hCD52}$ mice in the steady state were analyzed by flow cytometry. A majority of $CD25^+$ cells were hCD2 positive, but a substantial number of $hCD2^+$ cells were detected even in $CD25^-$ cells (18) (Figure 2A), which is consistent with the previous findings by the other group (19). Therefore, the following studies were performed using Kaede/$Foxp3^{hCD2/hCD52}$ mice, and $hCD2^+$ cells were considered to be Tregs.

To evaluate T cell migration from the skin in the steady state, the clipped abdominal skin of Kaede/$Foxp3^{hCD2/hCD52}$ mice was exposed to violet light as in Figure 1A, and 24 hours later, the draining axillary LN cells were subjected to flow cytometry. Consistent with the previous results (Figure 1D), a substantial percentage (0.83%) of photoconverted $CD4^+$ T cells were observed in the DLNs (Figure 2B). Among $hCD2^-$ non-Tregs and $hCD2^+$ Tregs, the frequency of Kaede-red cells was comparable (0.79% vs. 0.98%) (Figure 2C), and the frequency of Kaede-red cells was higher in the $CD44^{hi}$ memory subset than in the $CD44^{mid}$ naive subset (Figure 2C). In addition, Kaede-red $CD4^+$ cells included a higher percentage of Tregs (22.7%) than total $CD4^+$ cells (14.1%) (Figure 2D). In total $CD4^+$ populations, the number of $CD44^{hi}$ memory cells was lower than that of $CD44^{mid}$ naive cells in both non-Tregs and Tregs (Figure 2E). In contrast, consistent with Figures 2C and 2D, $CD44^{hi}$ memory cells were the major Kaede-red migrants from the skin among non-Tregs and Tregs (Figure 2E).

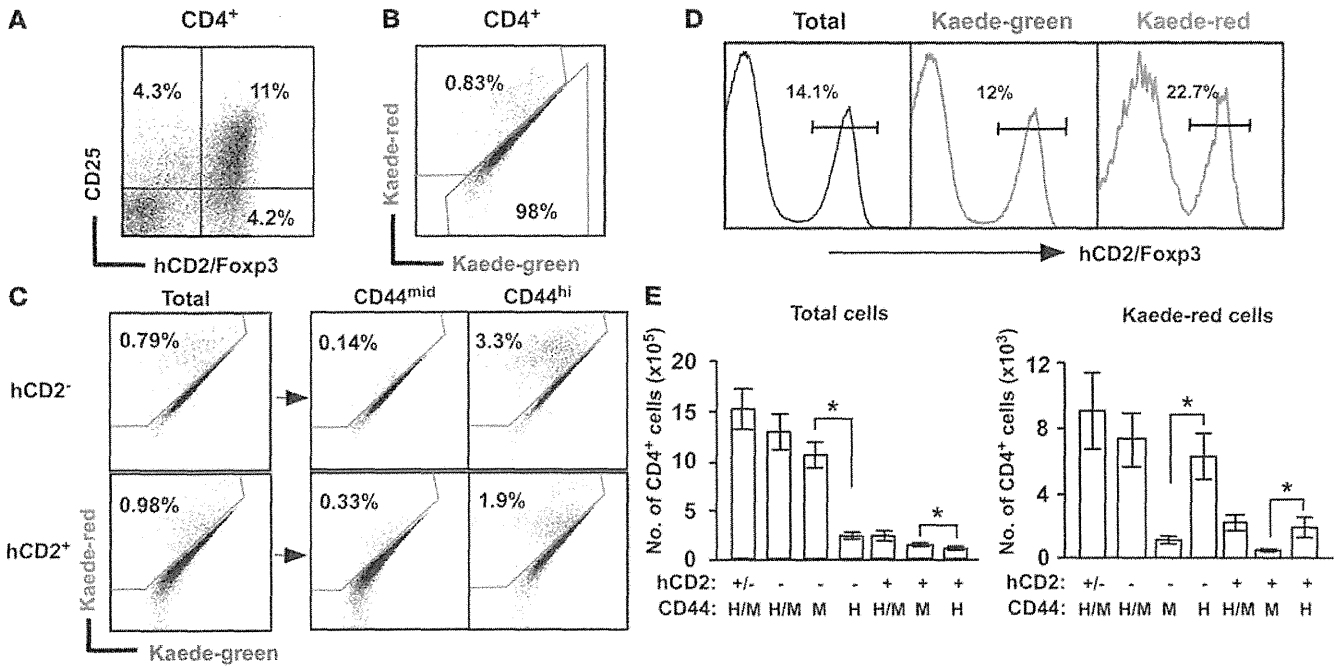

Figure 2

Migration of Tregs from the skin to DLNs. (**A**–**E**) The DLN cells of Kaede/Foxp3$^{hCD2/hCD52}$ mice photoconverted on the abdomen 24 hours prior were stained with CD4, CD25, and hCD2 mAbs. Shown here are the flow cytometric plots for hCD2/Foxp3 and CD25 staining among CD4$^+$ cells (**A**) and Kaede-red and Kaede-green expression on hCD2$^+$CD4$^+$ cells among skin DLN cells (**B**). (**C**) The DLNs and non-DLNs from the mice 24 hours after photoconversion were stained with CD4, hCD2, and CD44 mAbs and subjected to flow cytometry. (**D**) hCD2/Foxp3 expression in total (Kaede-red plus Kaede-green), Kaede-red, and Kaede-green CD4 cells was compared by flow cytometry. (**E**) The numbers of CD44^{mid} naive (M), CD44^{hi} memory (H), and naive plus memory (H/M) phenotypes of hCD2$^-$CD4$^+$ non-Tregs (–), hCD2$^+$CD4$^+$ Tregs (+), and total (hCD2$^-$ and hCD2$^+$; +/–) CD4$^+$ T cells in total CD4$^+$ (Kaede-red plus Kaede-green) cells and Kaede-red cells in the DLNs were counted. Data are presented as means ± SD and are representative of 3 independent experiments. Student's *t* test was performed between the indicated groups. $^*P < 0.05$. Numbers within plots or histograms indicate percentage of cells in the respective areas (**A**–**D**).

Treg migration from the skin during a cutaneous immune reaction. We tracked the extent of CD4$^+$ T cell migration from the skin during an immune response and sought to evaluate the role of CD4$^+$ T cells migrating from the skin. The dorsal skin of Kaede/Foxp3$^{hCD2/hCD52}$ mice was sensitized with 2,4-dinitro-1-fluorobenzene (DNFB), and 5 days later, the abdominal skin was challenged with DNFB. Two days after challenge, the abdominal skin was exposed to violet light for photoconversion, and another 24 hours later, the draining axillary LN cells were analyzed by flow cytometry (Figure 3A). The frequency of Kaede-red cells among CD4$^+$ T cells in the DLNs was increased up to 3% (Figure 3B) from that in the steady state (0.83%; Figure 2B). In addition, although 21% of total CD4$^+$ cells were Tregs, the number of hCD2$^+$ Tregs became comparable to that of non-Tregs in Kaede-red phenotype (49%; Figure 3, C and D). Again, the CD44^{hi} memory cells were major migrants from the challenged skin similarly to the steady state (Figure 3D and Figure 2E). The number of total CD4$^+$ T cells in DLN increased by 3-fold during contact hypersensitivity (CHS) compared with that in the steady state. However, the number of Kaede-red migratory non-Tregs and Tregs during CHS increased more drastically, by about 10- and 20-fold, respectively (Figure 2E and Figure 3D).

Consistent with increase of CD4$^+$ T cells migrating from the challenged skin into DLN, the numbers of both CD4$^+$ Tregs and CD4$^+$ non-Tregs were elevated when mice were sensitized and challenged compared with the steady state, and the ratio of Tregs to CD4$^+$ T cells during the immune response became higher than that in the steady state (Figure 3E). These results suggest that more Tregs than non-Tregs accumulate in the skin during the cutaneous immune response.

It is known that cutaneous dendritic cells migrate into the DLNs in a CCR7-dependent manner (20) and that in humans, most circulating Tregs express skin-homing receptors and CCR7 (21). To address whether skin T cells have the potential to migrate into the regional LNs, skin cell suspensions were obtained from the ears of mice sensitized on the abdomen and challenged on the ear with DNFB and applied to a transwell assay. The Tregs showed good chemotactic responses to CCL21 comparable to that of MHC class II$^+$ cutaneous dendritic cells (Figure 3F). Similar chemotactic activity to CCL21 was seen in CD4$^+$ non-Tregs (data not shown). Since the ratio of Tregs and non-Tregs in Kaede-red CD4$^+$ T cells in LNs was comparable to that in the skin at the time of photoconversion, Tregs and non-Tregs in the skin seem to have equivalent propensity to migrate to the DLN. In addition, we evaluated the CCR7 expression of Tregs in the skin before and after challenge and found that Tregs in the skin expressed CCR7 both before and after challenge and that the expression level of CCR7 of Tregs after challenge was slightly lower than that before challenge (Supplemental Figure 5).

Role of Tregs in the elicitation phase of CHS. As shown above, Tregs accumulate in the skin and they have the capacity to migrate to DLNs during the CHS response. These results prompted us to

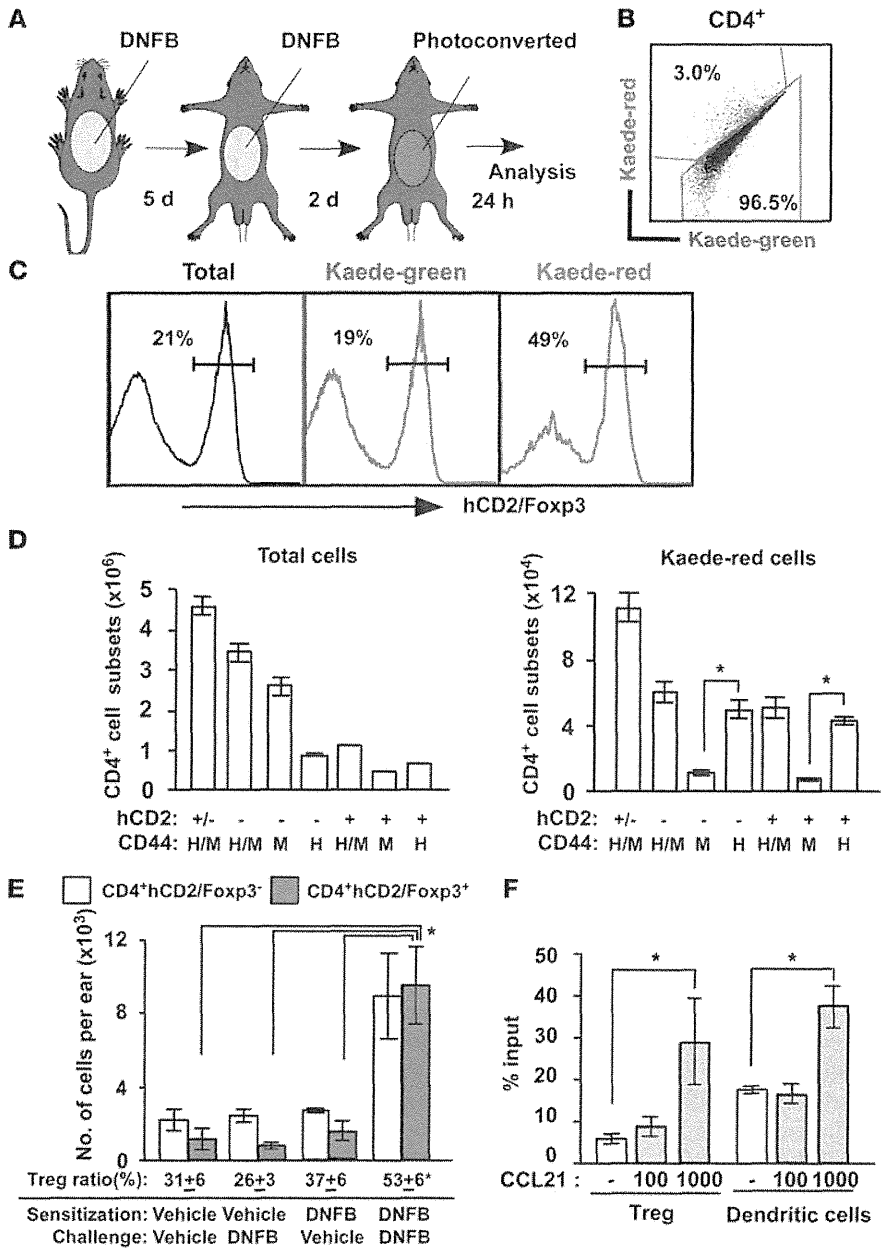

Figure 3

Cell migration from the skin to DLN during a cutaneous immune response. (**A**) Scheme of the experimental protocol is as follows: the dorsal skin of Kaede/Foxp3$^{hCD2/hCD52}$ was sensitized, and 5 days thereafter the abdominal skin was challenged. 2 days after challenge, the painted areas were photoconverted, and 24 hours after photoconversion, cells from the skin DLNs were analyzed by flow cytometry. (**B** and **C**) The frequency of Kaede-red and Kaede-green cells among CD4$^+$ cells, and the frequencies of hCD2/Foxp3+ cells in total, Kaede-green, and Kaede-red cells among CD4$^+$ cells were analyzed. Numbers within plots or histograms indicate percentage of cells in the respective areas. (**D**) The numbers of CD44^{mid} naive (M), CD44^{hi} memory (H), and naive plus memory (H/M) phenotypes of hCD2$^-$CD4$^+$ non-Tregs (–), hCD2$^+$CD4$^+$ Tregs (+), and total (hCD2$^-$ and hCD2$^+$; +/–) CD4$^+$ T cells among total CD4$^+$ cells and Kaede-red cells in the DLNs were counted. (**E**) Number of Tregs and non-Tregs in the skin. The mice were painted with DNFB or vehicle on the abdomen, followed by DNFB or vehicle application on the ears. The number of CD4$^+$ Tregs and CD4$^+$ non-Tregs and the percentage ratio of Tregs among CD4$^+$ T cells in the ears were measured. (**F**) Transwell assay. The number of hCD2$^+$CD4$^+$ cells and CD11c$^+$ cells of skin-cell suspensions from Foxp3$^{hCD2/hCD52}$ mice that migrated to the lower chamber was analyzed. Data are presented as means ± SD (**D**–**F**) and are representative of 3 independent experiments. Student's *t* test was performed between the indicated groups. $^*P < 0.05$ (**D**–**F**).

evaluate the role of Tregs in the cutaneous immune response. In a murine CHS model, we found that administration of Campath-1G Ab (a depleting Ab for the human CD52 antigen; ref. 22) resulted in a marked decrease in the number of Tregs in the DLNs and the skin, 1–3 days after injection (Figure 4A and data not shown). Kaede/Foxp3$^{hCD2/hCD52}$ mice were sensitized with DNFB on the abdomen and treated in the presence or absence of Campath-1G Ab. The ear thickness changes after the challenge on the ears were significantly prolonged by the treatment with Campath-1G Ab at each time point compared with in control mice (Figure 4B). This enhancement of CHS response by Campath-1G Ab was not observed when C57BL/6 (B6) wild-type mice were used, which excluded the possibility of the nonspecific effect of Campath-1G Ab (Supplemental Figure 6). In addition, the ear thickness changes of mice treated with control rat IgG were comparable to those treated without Campath-1G Ab (data not shown). These results demonstrate that Tregs play an important role in the challenge phase in terminating the CHS response.

Suppressive activity of Kaede-red and Kaede-green Tregs on T cell proliferation. To further determine the suppressive function of the Tregs migrating from the skin during the cutaneous immune response, Kaede-red and Kaede-green CD4$^+$ Tregs in the skin DLN were prepared as in Figure 3A and cocultured with regional LN cells from DNFB-sensitized mice. Antigen-specific T cell proliferation induced by 2,4-dinitrobenzene sulfonic acid (DNBS), a water-soluble compound with the same antigenicity as DNFB, was significantly inhibited by addition of 6×10^3 Kaede-red Tregs (Figure 4C). On the other hand, 8 times the number of Kaede-green Tregs was required to achieve a similar magnitude of inhibitory effect of the Kaede-red Tregs (Figure 4C). These data indicate that the skin-

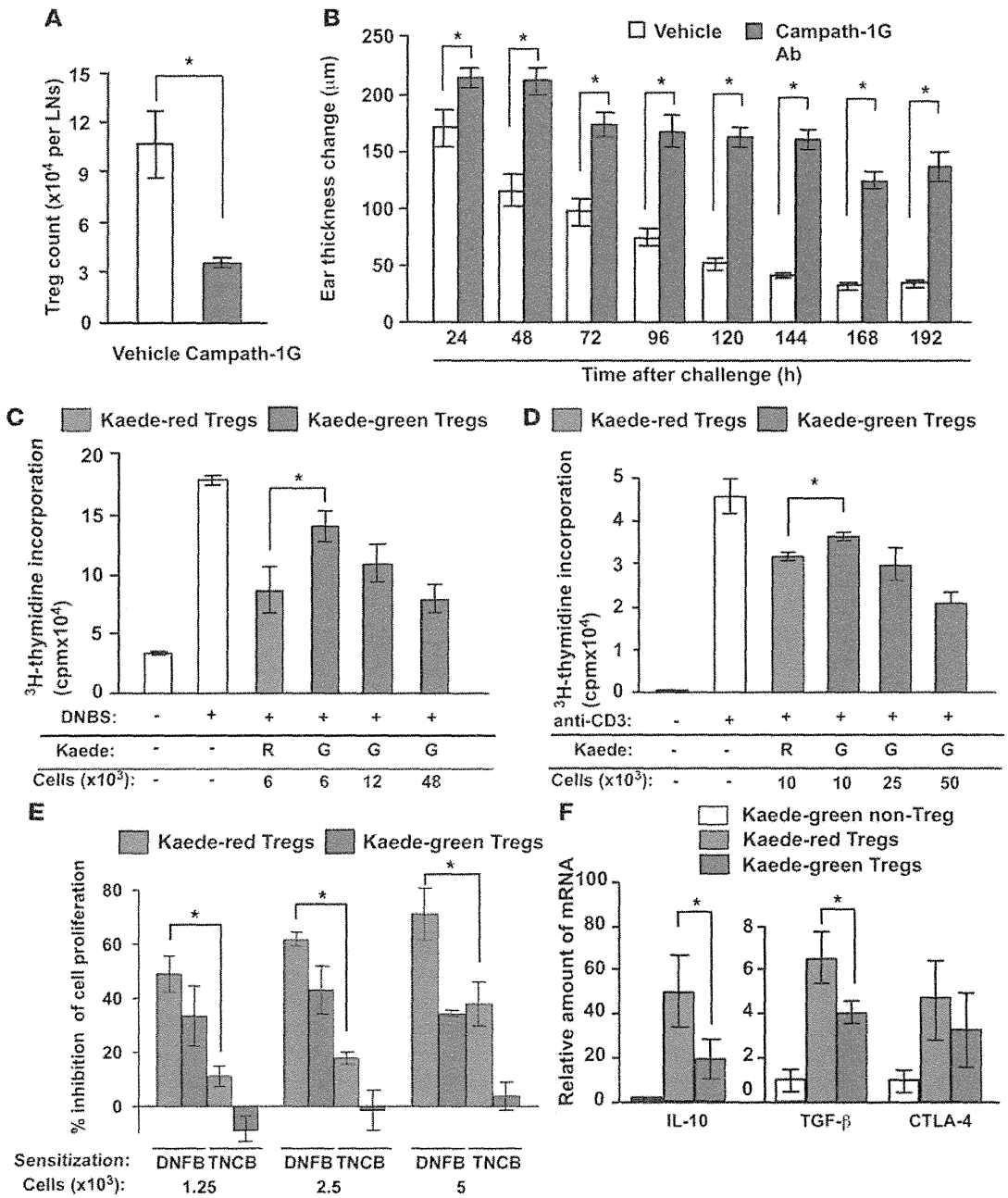

Figure 4

Enhanced ear swelling response by Treg depletion and immunosuppressive activity of Treg subsets on T cell proliferation in vitro. (**A**) The number of Tregs in the LNs after administration of Campath-1G Ab. (**B**) CHS: the Kaede/Foxp3$^{hCD2/hCD52}$ mice were sensitized, and injected with vehicle or Campath-1G Ab before challenge (n = 8 for each group). (**C**–**F**) Immunosuppressive activity of Tregs. Kaede-red and Kaede-green Tregs were sorted from the Kaede/Foxp3$^{hCD2/hCD52}$ mice, sensitized, challenged, and photoconverted. (**C**) Skin DLN cells of mice sensitized with DNFB were stimulated with DNBS in the presence or absence of Kaede-red Tregs or Kaede-green Tregs in vitro (n = 3). (**D**) Suppressive effect of Tregs in vitro. Kaede-red and Kaede-green Tregs were prepared as above and added to T cells stimulated with plate-bound anti-CD3 Ab. (**E**) Antigen specificity of Treg functions. LN cells from DNFB-sensitized or TNCB-sensitized mice were stimulated with DNBS or TNBS in vitro. Kaede-red and Kaede-green Tregs were added, and percentage inhibition of cell proliferation was evaluated as follows: (cell proliferation with DNBS or TNBS) – (cell proliferation with DNBS or TNBS in the presence of Tregs)/(cell proliferation with DNBS or TNBS) – (cell proliferation with vehicle) × 100. (**F**) Quantitative RT-PCR analysis on mRNA for *Il10* (IL-10), *Tgfb1* (TGF-β), and *Ctla4* (CTLA-4) of Kaede-red Tregs and Kaede-green Tregs. The expression of each gene was normalized by the expression of *Gapdh*, and those in Kaede-green non-Tregs were normalized to 1 (n = 3). Data are representative of 3 independent experiments and presented as means ± SD (**A**–**F**). *P < 0.05 between the indicated groups (Student's t test, **A**, **B**, **E**, and **F**; 1-way ANOVA followed by Dunnett multiple comparison test, **C** and **D**).

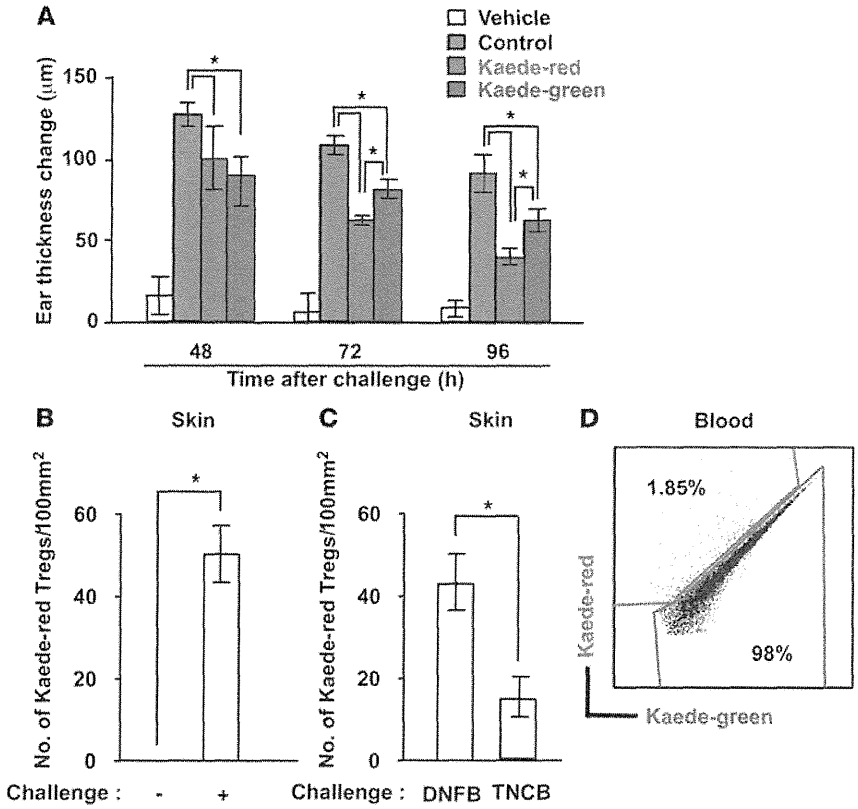

Figure 5

Immunosuppressive effect of Kaede-red Tregs in the skin. (**A**) Suppression of CHS response by Kaede-red Tregs. Kaede-red or Kaede-green Tregs (4×10^3 cells/ear) of Kaede/Foxp3$^{hCD2/hCD52}$ mice sensitized, challenged, and photoconverted as in Figure 3A were injected into ear skin of mice sensitized with DNFB 5 days prior. Immediately after injection, the mice were challenged, and the ear thickness change was measured at 48, 72, and 96 hours after challenge. (**B–D**) The mice were sensitized, challenged, and photoconverted as in Figure 3A. Twenty-four hours after photoconversion, 20 μl of 0.3% DNFB (challenge; +) or vehicle (challenge; –) (**B**) or 20 μl of 0.3% DNFB or 20 μl of 1% TNCB (**C**) was painted onto the ear. Twenty-four hours later, the ear skin and blood (**D**) were collected and dissociated for flow cytometry. The number of Kaede-red Tregs in the skin and the frequency of Kaede-red Tregs in CD4$^+$ T cell subset of the blood were evaluated (n = 3, each group). Data are presented as means ± SD and representative of 3 independent experiments (**A–C**). Student's t test was performed between the indicated groups. $^*P < 0.05$. Numbers within plots indicate percentage of cells in the respective areas (**D**).

derived Tregs have a stronger inhibitory effect on hapten-specific T cell proliferation than LN-resident Tregs. It should be noted that we might underestimate the inhibitory capacity of skin-migratory T cells relative to resident Tregs, since Kaede-green cells should have included the cells migrated from the skin before photoconversion and the cells that infiltrated to the skin after photoconversion and migrated to DLN.

We tested the effect of the Tregs on antigen-nonspecific T cell proliferation stimulated with membrane-bound anti-CD3 Ab. Kaede-red Tregs inhibited T cell proliferation more potently than did Kaede-green Tregs, and again a higher number of Tregs were required (Figure 4D) to obtain an extent of inhibition similar to that seen in Figure 4C.

To further evaluate the antigen specificity of Tregs in T cell proliferation, we isolated the DLN cells 5 days after DNFB or 2,4,6-trinitro-l-chlorobenzene (TNCB) sensitization and restimulated them with DNBS or trinitrobenzene sulfonic acid (TNBS), respectively, and added Kaede-red Tregs or Kaede-green Tregs prepared from the DLNs as in Figure 3A. Kaede-red Tregs inhibited DNBS-induced T cell proliferation more than Kaede-green Tregs (Figure 4E), as shown in Figure 4C. However, this antiproliferative effect was not seen when these Kaede-red or Kaede-green Tregs were added to TNBS-stimulated LN cells from the mice sensitized with TNCB (Figure 4E). In addition, in the criss-cross comparison, similar antigen-specificity was observed on TNCB-immunized Kaede-red Tregs (data not shown). We also analyzed mRNA expressions of inhibitory cytokines and surface molecules by quantitative RT-PCR. Kaede-red Tregs expressed higher mRNA levels of *Il10* and *Tgfb1* than Kaede-green Tregs (2, 3, 23) (Figure 4F). On the other hand, although there was no significant difference, Kaede-red Tregs tended to express higher mRNA levels of cytotoxic T lymphocyte-associated molecule-4 (*Ctla4*) than did Kaede-green Tregs (2, 3, 23) (Figure 4F). These results suggest that Tregs migrating from the skin have a more efficient suppressive potency on T cell proliferation with abundant inhibitory mediators and that this antiproliferative effect shows some antigen specificity.

Tregs recirculating from the skin inhibit local cutaneous immune response in situ. The strong ability of Kaede-red Tregs to suppress in vitro T cell proliferation prompted us to determine whether Kaede-red Tregs can inhibit a local cutaneous immune response in situ. Kaede-red or Kaede-green Tregs prepared as described (Figure 3A) were injected subcutaneously into the ears of mice sensitized with DNFB 5 days before, and the ears were challenged with DNFB. The DNFB-induced ear thickness change was suppressed by the injection of Kaede-red and Kaede-green Tregs at all time points (Figure 5A). It was noted, however, that Kaede-red Tregs suppressed CHS more than Kaede-green Tregs at 72 and 96 hours after challenge (Figure 5A).

Considering that Tregs function as a regulator for primed T cells, they should serve as suppressors at the challenged site. The above late-phase inhibitory action of Kaede-red Tregs raised the possibility that Tregs migrating from the skin can return to the skin and exert suppressive activity. Kaede/Foxp3$^{hCD2/hCD52}$ mice were sensitized, challenged, and photoconverted as in Figure 3A. Twenty-four hours after photoconversion, the left and right ears were rechallenged with DNFB and vehicle (Figure 5B) or TNCB (Figure 5C), respectively. Another 24 hours later, Kaede-red Tregs were observed in the ears challenged with DNFB, but not in those challenged with vehicle (Figure 5B). The ear rechallenged with a different hapten, TNCB, contained Kaede-red Tregs, but its number was lower than

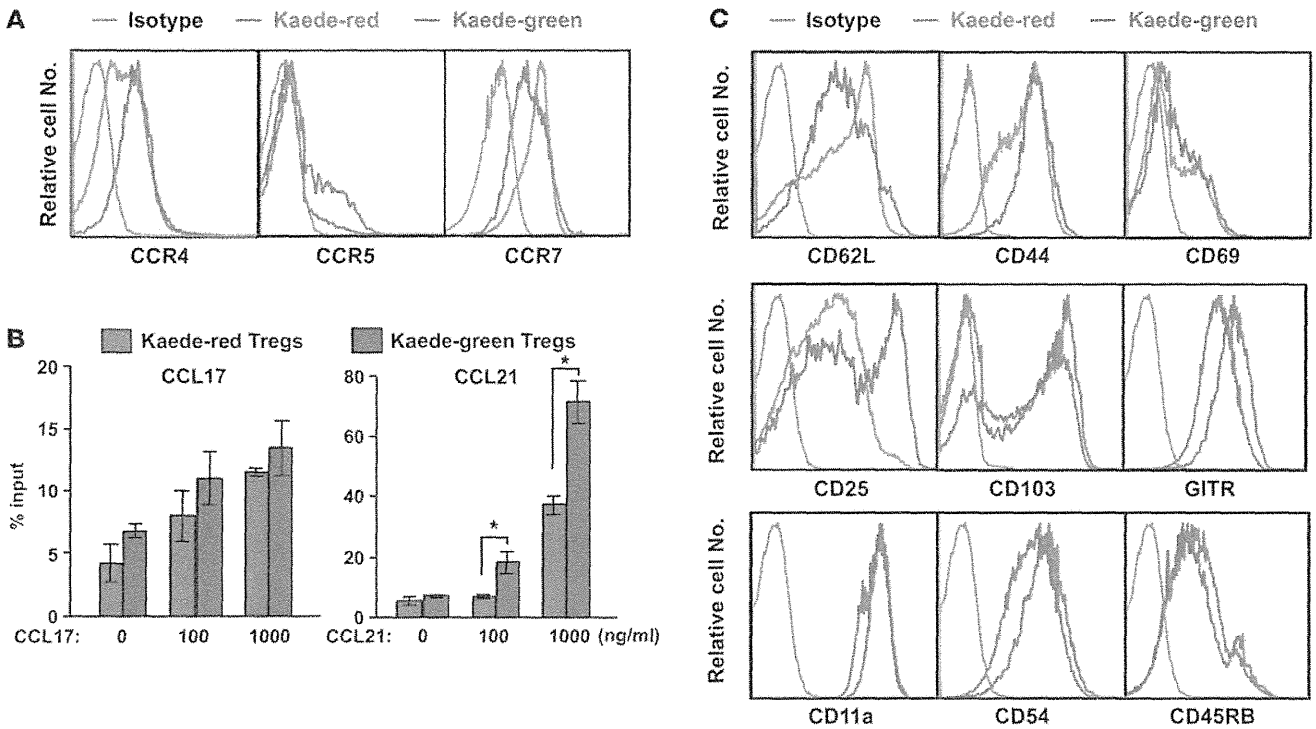

Figure 6

Surface molecule expressions on Kaede-red and Kaede-green cells. (**A**) Chemokine receptor expression. Skin DLN cells were prepared from the mice sensitized, challenged, and photoconverted as in Figure 3A. These LN cells were stained with isotype-matched control, CCR4, CCR5, and CCR7 mAbs, and the expression levels of Kaede-red and Kaede-green Tregs were evaluated by flow cytometry. (**B**) Transwell assay. DLN cells were transferred to the upper chamber of the transwell, and CCL17 or CCL21 was added to the lower chamber. The cells were incubated for 3 hours, and the numbers of Kaede-red and Kaede-green cells that migrated to lower chamber were analyzed by flow cytometry. Data are presented as means ± SD and representative of 2 independent experiments. Student's *t* test was performed between the indicated groups. $^*P < 0.05$. (**C**) Surface molecule expression. LN cells were stained with isotype-matched control, CD62L, CD44, CD69, CD25, and CD103 mAbs, and the expression levels were evaluated by flow cytometry. These data are representative of 3 independent experiments.

that of the ear rechallenged with DNFB (Figure 5C). In addition, Kaede-red Tregs were detected in $CD4^+$ cells of the blood 24 hours after rechallenge (1.79% ± 0.07%, average ± SEM, $n = 3$) (Figure 5D). Moreover, a previous report has suggested that LN cells migrate to the skin (24). We conducted an evaluation of this report by photoconverting DLNs. We sensitized the dorsal skin of mice with DNFB and challenged the abdominal skin with DNFB 4 days later. Two days after challenge, the DLNs of the mice were photoconverted and the ears were rechallenged with DNFB. Twenty-four hours later, the ears of the skin were analyzed by flow cytometric analysis. We found that a substantial fraction of $CD4^+$ $hCD2^-$ non-Tregs and $CD4^+$ $hCD2^+$ Tregs were Kaede-red positive (Supplemental Figure 7). These results suggest that the Tregs that egressed from the skin had a capacity to remigrate to the skin upon challenge.

It has been reported that the representative chemokine receptors essential for migration of lymphocytes into the skin and LNs are CCR4 and CCR7, respectively (9, 14, 25). In addition, CCR5 may be an important chemokine receptor for Tregs to migrate into the skin (26). Kaede-red Tregs expressed higher levels of CCR4 and CCR5 and a lower level of CCR7 than Kaede-green Tregs (Figure 6A). When the skin DLN cells prepared as in Figure 3A were applied to a transwell assay, Kaede-red Tregs showed good chemotactic responses to both CCL17, a ligand for CCR4, and CCL21, a ligand for CCR7, but the chemotaxis of Kaede-red Tregs to CCL21 was weaker than that of Kaede-green Tregs (Figure 6B).

We further analyzed the surface molecules of Kaede-red Tregs in the DLNs of Kaede/Foxp3$^{hCD2/hCD52}$ mice treated as in Figure 3A. Kaede-red Tregs expressed a lower level of CD62L but higher levels of CD44 and CD69 than Kaede-green Tregs (Figure 6C), suggesting that the skin-derived Tregs show a more memory-related T cell phenotype. Interestingly, Kaede-red Tregs contained a $CD25^{hi}$ fraction, which was barely perceptible in Kaede-green Tregs. In addition, Kaede-red Tregs expressed higher levels of CD103, an integrin important for T cell migration into the skin as well as CD11a and CD54, integrins induced upon activation, and a glucocorticoid-induced TNFR family–related gene/protein (GITR), another marker of Tregs (2, 27, 28) (2). However, the expression level of CD45RB was comparable between the Kaede-red and Kaede-green Tregs. These results suggest that Kaede-red Tregs are of the memory/effector phenotype (29) and have a higher potential to migrate to the skin than LN-resident Tregs.

Kinetics and surface phenotype of $CD25^{hi}$ Kaede-red Tregs. The above data (Figure 5A) suggest that Tregs migrating from the skin have a highly potent immunosuppressive capacity even in situ. One of the features of these skin-derived Tregs is the presence of a $CD25^{hi}$ subset (Figure 6C) that has not, to our knowledge, been thoroughly described before. Initially, we sought to characterize the localization of $CD25^{hi}$ Tregs and found that $CD25^{hi}$ cells were substantially detected in Kaede-red Tregs of the DLNs of mice pretreated as in Figure 3A but were only somewhat or marginally detected in